TIME-DEPENDENT RELIABILITY ASSESSMENT OF SEAWALLS SUBJECTED TO STOCHASTIC WAVES AND SEA-LEVEL RISE

A Thesis

by

VISHNU PRIYA JONNALAGADDA

Submitted to the Office of Graduate and Professional Studies of
Texas A&M University
in partial fulfillment of the requirements for the degree of

MASTER OF SCIENCE

Chair of Committee,	Arash Noshadravan
Committee Members,	James M. Kaihatu
	Daren B.H. Cline
Head of Department,	Robin Autenrieth

August 2020

Major Subject: Civil Engineering

Copyright 2020 Vishnu Priya Jonnalagadda

ABSTRACT

Sea walls play a major role in protecting the coastal regions from the raging waves and floods that can commonly occur due to storms and hurricanes. The rising sea levels and the increased number of storm events demand to re-examine the performance of the sea walls during their lifetime under future scenarios. The uncertainty is pervasive in this process stemming from stochastic nature and time variability of coastal forcing, as well as the various uncertain future scenarios of extreme climate events and sea-level rise (SLR). The objective of this research is to conduct an improved reliability-based assessment of coastal sea walls with the risk of overtopping as its primary failure mode. In our reliability analysis, we consider the uncertainty due to the stochastic nature of waves acting on the structure as well as the sea-level rise. The risk of overtopping failure is evaluated while incorporating the joint probabilistic description of the seawater level, significant wave height, and wave period under future hydraulic conditions. USACE (United States Army Corps of Engineers) SLR scenarios and USGS (United States Geological Survey) wave projections are used to account for the future hydraulic conditions. The uncertainty in the time-evolution of future sea level is quantified and systematically incorporated by constructing a stochastic model based on the inverse Gaussian process using the data from the USACE SLR projection scenarios. A time-dependent reliability-based framework is formulated to propagate different sources of uncertainty into the quantification of the probability of failure of sea walls. Specifically, we used the Galveston sea wall, which is a reinforced concrete curved seawall, as the case study. We explored the sensitivity of the

probability of overtopping to different sources of uncertainty. It is identified that wave height plays a crucial role in causing overtopping failure than all the other parameters. The outcome of this research will lead to knowledge and improved modeling framework that helps policymakers and infrastructure operators to characterize the risk of failure and resilience of coastal defense structures under various uncertain future scenarios and identify the adaptation or mitigation strategies that result in maximum resilience gain in the system.

DEDICATION

To my parents, Sailaja and Naresh Kumar Jonnalagadda, this would have not been possible without you. Thank you for everything.

ACKNOWLEDGMENTS

First and foremost, I would like to express my deepest gratitude to my research advisor, Dr. Arash Noshadravan, for his constant support, his endless patience, and his invaluable suggestions on every aspect of this work. This thesis would not have been possible without his guidance. I would also like to thank my committee members, Dr. James M Kaihatu and Dr. Daren B.H. Cline, for their comments and suggestions for improvement of this work.

I am sincerely thankful to my friends Stuti Sakhi and Mounika Kunduru for their suggestions and insight, especially at times when I needed it the most. I also would like to thank Bharat Kalivarapu for his continuous support and trust in me.

Finally, a huge thank you to my parents and grandparents who have always pushed me to seek boundaries I thought were impossible for me. As well as the department faculty and staff for making my time at Texas A&M University a memorable one.

CONTRIBUTORS AND FUNDING SOURCES

Contributors

This work was supported by a thesis committee consisting of Dr. Arash Noshadravan and Dr. James M Kaihatu of the Department of Civil and Environmental Engineering and Dr. Daren B.H. Cline of the Department of Statistics.

All other work conducted for the thesis was completed by the student independently.

Funding Sources

There are no outside funding contributions to acknowledge related to the research and compilation of this document.

NOMENCLATURE

SLR	Sea Level Rise
USGS	United States Geological Survey
USACE	United States Army Corps of Engineers
NOAA	National Oceanic and Atmospheric Administration
IG	Inverse Gaussian
U.S.	United States
RCP	Representative Concentration Pathway
EM	Expectation Maximization
RSLR	Relative Sea Level Rise
CDF	Cumulative Distribution Function
PDF	Probability Density Function

TABLE OF CONTENTS

Page

LIST OF FIGURES

Page

1. INTRODUCTION

1.1. Motivation

In today's world, climate change is inevitable and rising sea levels and increased sea storminess are its most significant outcomes. Due to exacerbated environmental conditions and sea-level rise, coastal structures like seawalls which act as the first lines of defense from coastal hazards are subjected to high risk. This risk on the seawalls includes an increased rate of occurrence of overtopping and a high magnitude of hydrodynamic forces acting on the structure. Given that a large percentage of the population lives in the coastal regions, threats like flooding, shoreline erosion, and hazards from storms are getting amplified. Waves of high significant wave height can easily cause overtopping failure and due to their stochastic nature, it is important to accurately incorporate this variable in the risk analysis of seawalls. Figure 1 is plotted with wave height data from Erikson et al. (2016) for the year 1987 from the Gulf of Mexico region on the y-axis and time in hours on the x-axis, and it represents the stochastic nature of wave height data. The rising sea levels have the potential to easily imply the flooding impact of a less probable high-intensity storm event to a high probable low-intensity storm event. This makes the sea level rise another important variable when assessing the risk of coastal structures. This motivated our study on risk assessment of seawalls. Especially we have taken into consideration the Galveston seawall due to the high relative sea-level rise in the region. It is inferred from the studies that along the upper Texas coast the sea levels are rising more rapidly than worldwide because some coastal lands are sinking. As sea level

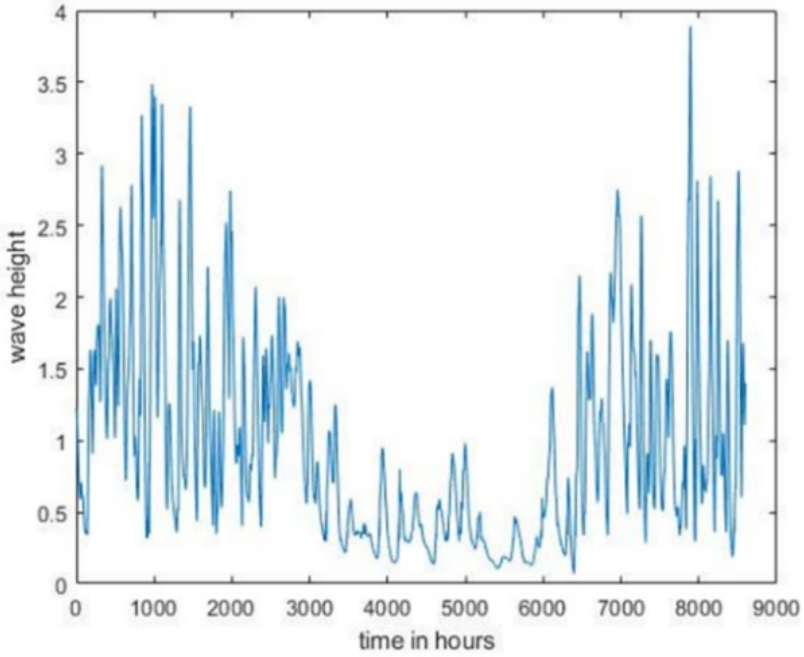

Figure 1 Graphical representation of wave height data for the year 1987 from the Gulf of Mexico region obtained from the USGS data source

rises, coastal areas become more vulnerable to storms and related floods. For example, a 0.91-m rise in sea level would enable a 15-year storm to flood many areas that today are only flooded by a 100-year storm. Land subsidence is a very significant problem along the Texas coast specifically in Galveston bay. Due to this land subsidence, Galveston bay is subjected to relative sea-level change. When the local level of the ocean relative to land is changing due to ocean rise or land subsidence, such a change is called relative sea-level change. This will become a pressing problem in this region given to the rate of sea-level rise. This has driven the study performed by Yoskowitz et al. (2009) who have modeled two scenarios of relative sea-level rise for the Galveston region and its surrounding counties for 100 years period. These regions are

well populated and significantly large. They have considered a 0.69 m rise and 1.5 m rise as the two scenarios. Their main objective is to estimate the impact of the two sea-level rise scenarios on the number of households. They have also estimated the expected number of buildings damaged, economic loss due to infrastructure damage, the effect on solid waste and industrial sites, and the impact on water treatment plants. They have concluded that under the 0.69 m rise the Galveston County alone will have 78% of its total households displaced. In the case of a 1.5 m rise, 93% of households will be displaced. It is also estimated that in the case of 1.5 m rise there is a possibility that more than 98 thousand households will be displaced, and 75 thousand buildings will get damaged. A total of 12.5 billion economic losses are calculated for the Galveston region. The effect of sea-level rise on the socio-economic level is profound. Similarly, the effect on public facilities, industrial sites, and waste management sites is highly significant. According to their study, it is calculated that around 23 sites will be impacted when there is 0.69 m rise and around 33 sites would be impacted under the case of 1.5m rise. In 2008 Texas has seen a powerful hurricane called Ike. So, in this study, they have calculated the economic damage if the same hurricane comes when there is a 0.69 m sea-level rise. They calculated that there would an additional 1.7 billion in damages for the total damages already caused. These results show us the expected impact of relative sea-level rise in the Galveston region under two different cases and show us the importance of studying the long-term impacts of climate change and sea-level rise in Texas.

Given the uncertainties and the risks involved in climate change, stochastic waves, and sea-level rise scenarios: probabilistic, risk analysis, and reliability methods give much leverage in solving problems surrounding these issues. So, in this study, the risk of overtopping failure was calculated by analyzing the joint probability of seawater level, significant wave height, and wave period also under future hydraulic conditions due to climate change. A reliability-based framework was formulated to address these uncertainties and to find out the probability of failure of the seawall.

1.2. Objectives

Based on the motivation to address the risks associated with seawalls, this work aims to conduct an improved reliability-based assessment of coastal sea walls with the risk of overtopping as its primary failure mode. Performance evaluation of seawalls under future scenarios had become critical given to the imminent effects of rising sea levels and the increased number of storm events. The proposed time-dependent reliability assessment model can quantify the uncertainties stemming from stochastic nature and time variability of coastal forcing, as well as the various uncertain future scenarios of extreme climate events and sea-level rise (SLR). The outcome of this research will create knowledge through improved modeling framework that informs policymakers and infrastructure operators to characterize the risk of failure and resilience of coastal defense structures under various uncertain future scenarios. This knowledge can support the decision in identifying adaptation or mitigation strategies that result in maximum resilience gain in the system.

The specific objectives are as follows:

1. Explore and integrate different data sources such as NOAA, USGS, and USACE for improved quantification of uncertainty in parameters and functions describing the reliability of sea walls.
2. Construct stochastic descriptions of future wave characteristics and rising sea levels to propagate the associated uncertainty into limit state functions
3. Use this development to study the time-dependent reliability of the Galveston sea wall under uncertainty in future hydraulic conditions and different sea-level rise scenarios.

1.3. Literature Review

The coastal structures are subjected to uncertain conditions like stochastic waves and rising sea levels. This makes the coastal structures vulnerable and prone to high risk. Reinforced concrete seawalls, in general, are under high risk of overtopping failure and structural deterioration failure. This led to many research studies on risk assessment of coastal structures subjected to uncertain conditions. Below are some relevant research studies on risk assessment of coastal structures.

Mehrabani et al. (2015) have presented a method for calculating the probability of failure of coastal defense structures due to overtopping. They have identified that a lot of research is done for risk assessment of coastal structures, but the uncertainties associated with sea-level rise and significant wave height are not incorporated into the study. So, in this study, they have considered the joint probabilistic nature of hydraulic variables like seawater level and significant wave height. To predict the future probability of failure they

have used the UKCP09 climate projection scenarios to incorporate the future hydraulic variables in the model. Identifying the time-dependent nature of hydraulic variables, they have used time-dependent reliability analysis to find the probability of failure of coastal defense structures. The main causes of overtopping failure are a combination of sea-level rise and waves with high significant wave heights. It is stated that sometimes waves with extreme significant wave height can alone cause overtopping failure. This emphasizes the importance of considering joint exceedance of significant wave height and seawater level as an important factor in designing coastal defense structures. They used Generalized Pareto Distribution (GPD) and Generalized Extreme Value (GEV) distributions to fit the data and analyze the results for a better understanding of the model. They have applied this model as a case study on a sea wall in North Wales. They have analyzed the overtopping failure of the seawall over time by utilizing the future projections data. They have clearly shown the impact of sea-level rise by plotting the rate of occurrence of overtopping failure with time with and without sea-level rise. The frequency of overtopping is high in the case where sea level rise is considered. They concluded that sea-level rise and significant wave height play an important role in assessing the risks of coastal structures.

Burcharth et al. (2015) presented the design, construction, and performance of the main breakwater of the new outer port at punto Langosteira, La Coruna, Spain. In the design of a coastal structure like a breakwater, initially, model testing was performed and then the design is finalized based on the reliability analysis. Detailed reliability analysis was performed to identify the safety levels of the various parts of the structure as a basis

for a more detailed design. The reliability analyses demanded that the uncertainties and scatter in the model test results were considered. For this reason, the model tests were repeated several times to obtain reliable expectation values and coefficients of variation of the parameters. And then a reliability analysis of the completed cross-section was performed. They have used the Monte Carlo simulation technique to obtain the failure probabilities for the failure modes Sliding, Slip failure, Main armor damage initiation, Main armor failure, Toe berm damage initiation, and Toe berm failure. They have assumed that the occurrence of the storms follows a Poisson distribution. From Monte Carlo simulations using 10,000 randomly chosen wave height values the failure probabilities within 50-year service life were obtained. No damage has been observed to any part of the structure even though it faced some severe storms. In the outer low- crested part of the breakwater, some settlements of cubes due to compaction of the front slope armor occur leaving openings in the transition between the single-layer and the double layer of cubes.

Chen and Mehrabani (2019) proposed a time-dependent reliability model to assess the risk faced by coastal defense structures. They emphasized the impact of climate change on sea level and significant wave height. Using this model, they can predict the future performance characteristics of coastal defense structures. Earth sea dikes are taken into consideration for this model. Overtopping and soil piping are identified as important failure modes for earth sea dikes. As these depend and vary with time, modeling them as a time-dependent reliability problem is adopted in this paper. The piping of soil, in turn, increases the frequency of overtopping as the structure loses its crest freeboard. They have modeled this as a time-dependent Markov process. The reliability model gives the results

concerning the probability of failure due to risks like overtopping and soil seepage. They are utilizing the results from the time-dependent reliability model as a base to arrive at optimum maintenance strategies. A multi-objective optimization method is used to make strategic maintenance plans by establishing an optimum maintenance solution space. In this, different samples are presented, and each solution has its deterioration rate, risk unit, the cost for maintenance, and the time interval between maintenance schedules. A solution from the sample space can be selected based on the conditions of the coastal defense structure. Properly scheduled maintenance and inspection plans help to reduce the risks faced by coastal defense structures and increase their performance in the long run. Earth sea dike at Thames estuary is chosen as a case study to apply this model. From the results, they have concluded that the effect of water levels and wave height on the failure of coastal structures is significant in the future given to sea level rise and climate change. The probability of failure of the coastal defense structures increases in the future due to the combined effect of overtopping and soil piping. The optimum maintenance strategy helps maintenance workers to utilize the resources properly and reduce the risks faced by coastal defense structures.

Li et al. (2005) presented a method to assess the serviceability of corrosion affected concrete structures. They point out that cracking and deflection causes the structure to lose its serviceability and can lead to the ultimate failure mode eventually, so they proposed this method to assess such risk. They proposed a performance-based methodology and used time-dependent reliability methods to evaluate the probability of failure. In this paper, they have used the theory of mechanics and experimental data to develop the

models of structural response. For structural response, they have used models like crack width and deflection. They introduced a deterioration function to account for an increase in deflection even under constant load. They have concentrated on corrosion-induced cracking and deflection and applied it to flexural members as an example. Using this method, they can determine the time for a structure to become unserviceable and it will in turn help to determine the time for maintenance scheduling. It is concluded that cracking is dominantly affected by corrosion rate which in turn is measured by corrosion current density and a corrosion affected structure can become easily unserviceable due to cracking before excessive deflection can happen. They have identified that correlation exists between two points in time of deflection deterioration. They concluded that this model can serve as a tool for engineers and maintenance workers for cost-effective and better planning of maintenance works of corrosion affected structures.

Lounis and Amleh (2004) proposed a reliability-based method to predict the chloride ingress and reinforcement corrosion of aging concrete bridge decks. It is identified that chloride-induced reinforcement corrosion is a pressing problem for reinforced concrete structures. Due to this corrosion, the strength of the structure is reduced and therefore leading to a reduction in its safety and serviceability. So, in this paper, they have presented probabilistic approaches for predicting the service life of concrete structures with an emphasis on predicting the chloride concentration at the steel and the corrosion initiation time and propagation time. They have considered the uncertainties that might arise in the corrosion process and physical modeling along with statistical and decision uncertainties. They have applied this model on the Dickson bridge

in Canada to observe its results. This approach helps in assessing the safety and serviceability of deteriorating concrete structures to ensure that the probability of failure is kept at an acceptable level. They conclude that a reliability-based prediction of the service life of deteriorating concrete structures provides an adequate decision support tool at both the initial design stage and during the operation and maintenance stage. The implementation of such an approach allows control of the safety and serviceability of the structure throughout its service life and results in a low life cycle cost.

Li and Zhao (2010) proposed a time-dependent risk assessment method for quantifying the risk faced by coastal defense structures. They have considered a reinforced concrete sea wall for applying this model. The two main types of failures for a reinforced concrete sea wall are overtopping failure and structural deterioration failure. Structural deterioration is a specific problem in reinforced concrete coastal defense structures due to reinforcement corrosion. Reinforcement corrosion leads to a decrease in structural capacity and thereby making the structure susceptible to damage due to aggressive waves acting upon the structure. They have identified that due to sea-level rise and unfavorable environmental conditions the risk on coastal defense structures is increasing with time. So, they have proposed a time-dependent reliability model to assess the risk. For the overtopping failure mode, they have considered that Poisson renewal is best suited to model the stochastic high-intensity waves. A limit state function is established to evaluate the overtopping probability of failure. It contains permissible discharge volume as the acceptable limit of the load and discharge volume is the actual load. They have introduced a deterioration model to account for sea water-induced steel reinforcement corrosion. The

limit state function established to evaluate the probability of failure due to structural deterioration contains the flexural capacity of the seawall as the acceptable limit of the load and the overturning moment on the structure caused by wave action as the actual load. The failure of the structure can happen even if either of overtopping failure or structural deterioration failure happens so the series system from the system reliability concept is adopted in this paper to find out the total probability of failure of the structure. They have considered a reinforced concrete vertical sea wall as a case study to apply this model. They have concluded that significant wave height, seawater level, acceptable discharge volume, and height of seawall are important factors when assessing the risk of coastal defense structures. The unfavorable environmental conditions and the sea level rise is increasing the risk faced by coastal defense structures. They have also identified that the risk of structural failures increases faster than the risk of wave overtopping in reinforced concrete vertical seawalls.

Ye and Chen (2014) investigated the use of the inverse Gaussian process as a degradation model. They state that the gamma process and wiener process are not sufficient to describe or fit all the degradation data. The inverse gaussian process has monotone paths similar to the gamma process. Random effects and explanatory variables can be included in the inverse gaussian process. Random effects are used to incorporate the heterogeneities that commonly occur in degradation problems. The authors have identified that the less usage of the inverse gaussian process is due to its unclear understanding. So, they have clearly emphasized on the physical meaning of the process and proved the convergence of the inverse gaussian process to compound Poisson process,

this provides a strong proof that inverse gaussian process can be used as a degradation model. The different inverse gaussian random effect models they have explained in this paper are random drifts model, random volatility model, and random drift volatility model. In this paper, they have also explained the statistical inference of parameters for the random-effects model and also how to choose among the different models. They have applied this model on an example problem to show the effectiveness of the inverse gaussian process and concluded that the inverse gaussian process is similar to the gamma process, but it is much more adaptable.

Liu et al. (2014) developed a reliability model for systems with multiple degradation processes using inverse gaussian process and copulas. Continuous degradation processes are usually modeled by stochastic processes. In general wiener and gamma processes are used for modeling degradation processes. It is identified that when using wiener process the degradation paths are necessarily not monotonic. It is recognized that only two, wiener, and gamma processes are not sufficient to describe all kinds of degradation processes. In this paper, they have modeled the monotonic degradation process using the inverse gaussian process. They have considered the inverse gaussian process with time scale transformation and random drift to incorporate heterogeneous degradation rates that arise in the product population. To systematically characterize the joint distribution of multiple degradation processes they have used copulas. To estimate the unknown parameters involved in the inverse gaussian process and copulas they have used the EM algorithm with a two-stage procedure. After estimating the parameters, they have performed a simulation study to determine the quality of the estimators. They used

the example of a crack growth problem to demonstrate their model in which they have considered two cracks as crack A and crack B representing multiple degradation processes. They have compared the results obtained from their model with a numerical example and concluded that their model is fitting when the degradation path is nonlinear. They concluded that their model is helpful in analyses involving multivariate degradation data. Their model is better than the common multivariate distribution model because in the multivariate distribution model there is a limitation of the same marginal distribution and it can only describe linear correlation.

Mehrabani and Chen (2016) performed Markov chain modelling for the life cycle performance assessment of coastal defense structures. They state that it is important to evaluate the condition of coastal defense structures given the effects of global warming and with the aging of coastal defense structures it is important to make strategic maintenance plans to protect them from structural deterioration and sea-level rise. So, in this paper, they have proposed a model to assess the performance of coastal defense structures in the future. They have considered overtopping, settlement, and deterioration of coastal defense structures for assessing their performance over time. They have used the Markov chain to assess coastal defense structures. For Markov chain modeling they have developed transition probabilities basing on condition grades of coastal defense structures which are established through visual inspection. They have considered the case of different condition grades at a time and modeled stochastic deterioration of the structure transitioning between different condition grades. They have applied their model on an earth sea dike to observe the results. From the results, it is identified that the performance

of coastal defense structures can be established from condition grades basing on the proposed method. This will help in making efficient maintenance plans and also fragility curves can be generated which will help in making risk cost maintenance decisions.

From the studies, it is identified that due to the time-variant and stochastic nature of waves and sea-level rise, a time-dependent reliability method would be appropriate to address risk assessment of coastal structures. Sea level rise is an important factor in assessing the failure probability of coastal structures. Sea level rise projections in the future in most of the cases are presented as different scenarios. It is identified as a potential research objective to quantify the uncertainty that arises due to the presence of different sea-level rise scenarios. It is also identified that most of the research is performed on sloped or vertical seawalls. Basing on the literature review, a curved seawall is chosen as a case study to perform improved time-dependent reliability assessment.

2. DATA COLLECTION AND ANALYSIS

It is identified that for real-time risk analysis of a sea wall, parameters like seawater level, wave height, and wave period are important terms. It is essential to have the appropriate data sources and analyze this data so that it can be properly incorporated into the risk analysis model. One of the objectives of this research is to explore and integrate different data sources such as NOAA, USGS, and USACE for improved quantification of uncertainty in parameters and functions describing the reliability of sea walls.

2.1. USGS Wave Projections

Recognizing the requirement for wind and wave projections Erikson et al. (2016) performed a detailed study in which they have used wind data from four different global climate models to simulate historical and future wave parameters by using the wave watch III model and this is performed under the influence of two climate scenarios. The two climate scenarios they have taken into consideration are the Representative Concentration Pathways (RCP) 4.5 and RCP 8.5, the prior represents a medium emission scenario and the later represents a high emission scenario. Under these two climate scenarios, they have calculated the wind data using the four different global climate models and used this wind data as input for the wave watch III model to generate wave data. Through their study, they have made available time-series data of significant wave height, wave period, wave direction, wind speed, and wind direction for the periods 1976-2005, 2026-2045, and 2081-2099/2100. They have considered various locations all along the U.S. coasts at which the data is made available. It is evident that water levels and wave parameters play

a crucial role in driving extreme weather conditions, so this data is highly useful in our study of risk analysis of a sea wall. In the web tool provided according to our requirement we can select different parameters, periods, climate scenarios to retrieve the data of a location. These data are available for download in both ASCII and NetCDF formats. If it is in the NetCDF format, data can be obtained using software like Panoply. (2020).

2.2. USACE Sea Level Rise Scenarios

Determining the importance of the rising sea levels USACE developed a web-based tool called sea-level change curve calculator. This tool helps in viewing the USACE and some other reliable sea-level rise scenarios for any tide gauge station that is part of NOAA (Huber and White.(2017)). In this tool on the right side we can see the various stations all around the U.S. and on the left side we can see the various options available to make our selection. We can choose the location, output units, output datum, etc. according to our requirement and visualize the output sea level rise curves.

2.3. NOAA Water Level Data

National Oceanic and Atmospheric Administration (NOAA) provides water level data at various coastal stations all-around U.S. NOAA's Tides and Currents website, developed and supported by the Center for Operational Oceanographic Products and Services (CO-OPS), provides the water level data. Through this, we can access both historical and current data on an hourly or 6-minute interval basis according to the options we choose. We can choose various options according to our requirement to access the water level data from (NOAA). We can choose the period during which we require the data, datum, units, interval, and also the time zone to obtain the data.

2.4. Data Analysis

USGS, NOAA, USACE provide excellent data sources for wave heights, wave periods, water levels, wind speed and directions for many U.S. coastal locations. After careful selection of the data, the next step is to analyze the data to determine its characteristics. This step is required for improved quantification of uncertainty in parameters. In this study, it is important to understand the probability distribution of the data. Basing on the original data we can assume different probability distributions and can conclude a distribution through the goodness of fit tests. Some goodness of fit tests are the K-S test, A-D test, etc. Probability plots can also be used to identify the distribution of the data. Another property of data that can be checked is the correlation between different parameters. Understanding the correlation between parameters is useful as it helps in predicting the value of one variable by using the other variable. When we are dealing with time-series data stationarity is an important property to check. When the statistical properties of data do not vary with time then it is defined to be stationary. Identifying properties like probability distributions, correlation, stationarity will be immensely helpful in making an accurate risk analysis. We used parametric distributions to find out the probability distributions of the data. It can be observed in Figures 2 and 4 that significant wave heights and wave periods follow Weibull distribution. From figure 3 we can see that seawater levels follow the normal distribution. The motivation for considering Weibull distribution for wave height is also strongly supported through (Muraleedharan et al., (1993), Muraleedharan et al., (1998)).

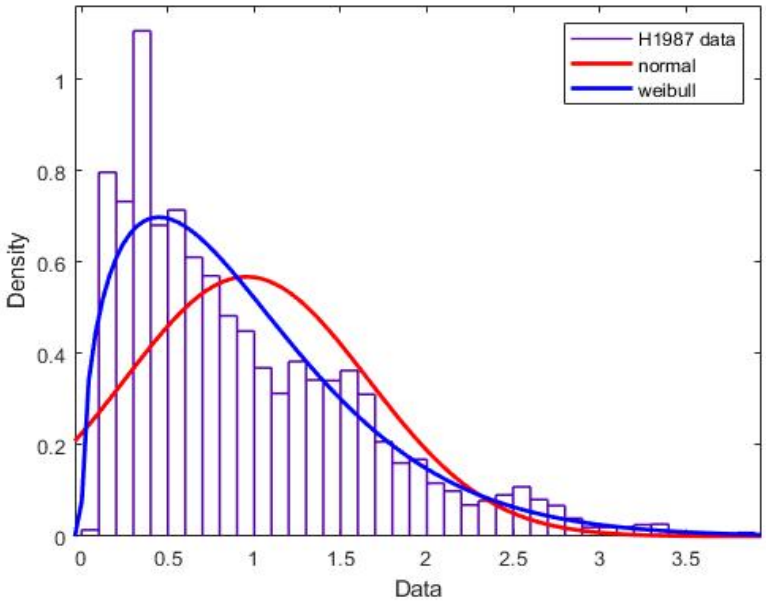

Figure 2 Distribution fitting for wave height data for the year 1987

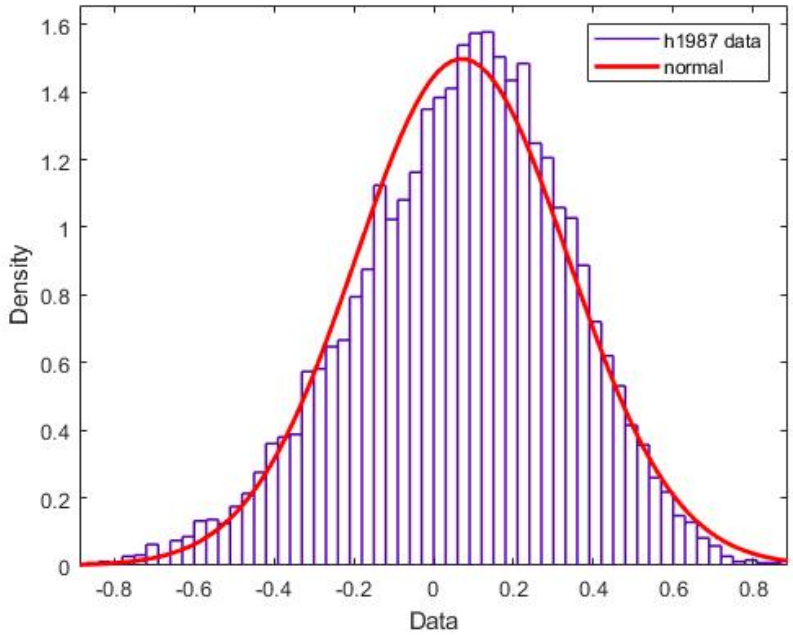

Figure 3 Distribution fitting for water level data for the year 1987

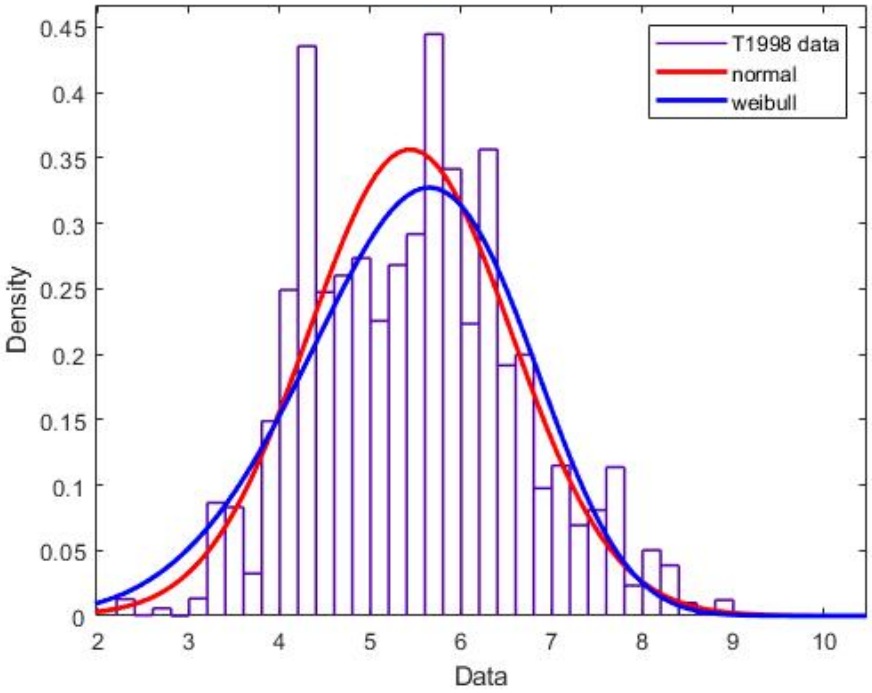

Figure 4 Distribution fitting for wave period data for the year 1998

A good amount of correlation is also observed between seawater level, significant wave height, and wave period which is represented in figure 5. It is also observed that the wave significant height, period, and water levels over time are stationary which can be seen in figures 6, 7, 8 which are plotted using the software Origin (Pro). (2020).

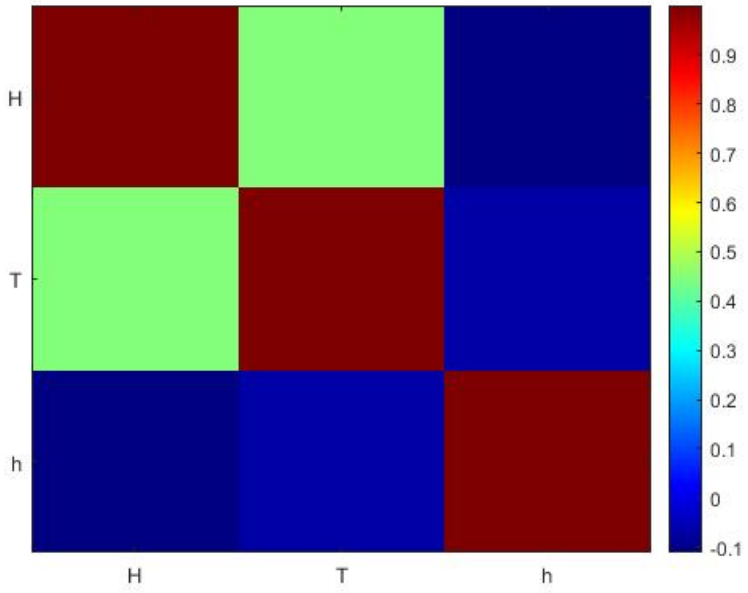

Figure 5 Correlation matrix of wave height(H), water level(h) and wave period(T) data

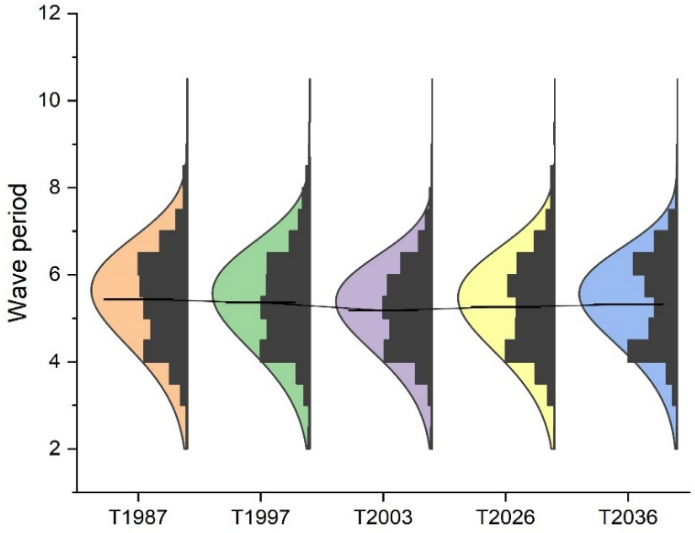

Figure 6 Stationarity of wave periods

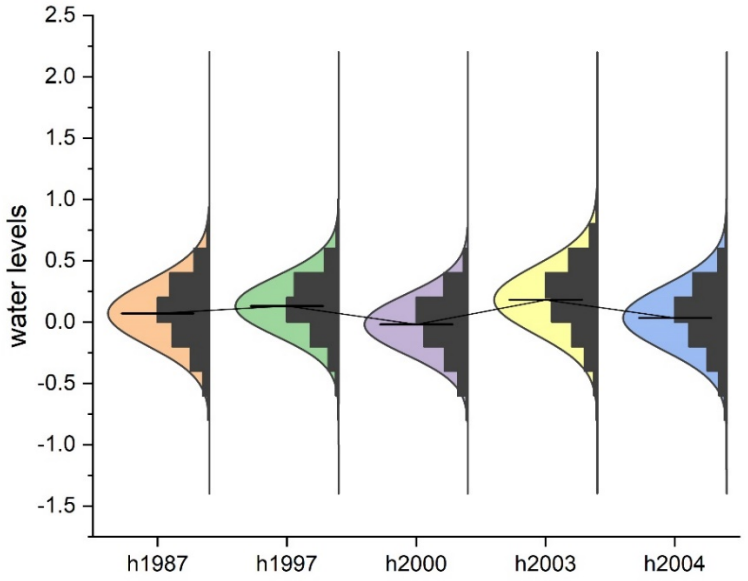

Figure 7 Stationarity of water levels

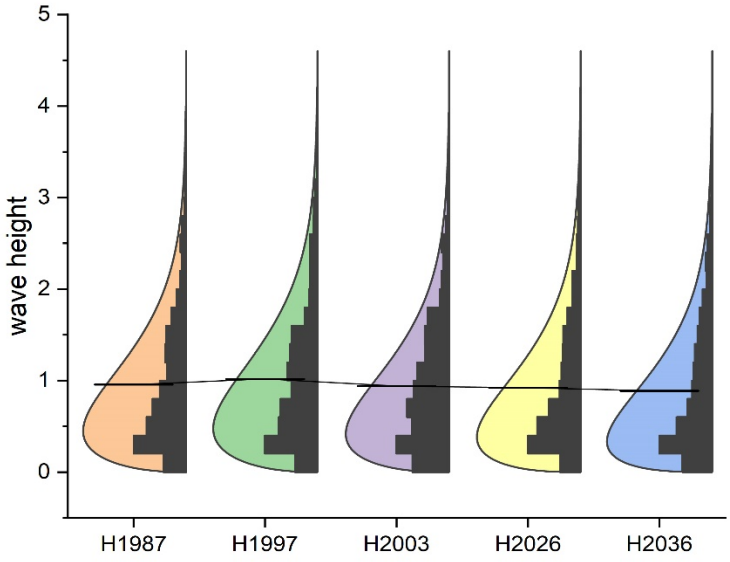

Figure 8 Stationarity of wave height

2.5. Copulas for Joint Probabilistic Description of Correlated Data

Copulas are useful when we want to stimulate correlated data. Abe Sklar introduced the concept of copulas and it is after him the Sklar's theorem is named. According to this theorem, if Z is a joint distribution function with continuous margins H_1, H_2... H_n, then there exists a unique copula C such that, for all x_1, x_2..., xn in R,

$$Z(x_1, x_2, x_{3,\dots} x_n) = C(H_1(x_1), H_2(x_2), \dots . . H_n(x_n)) \quad (2.1)$$

A copula can be defined as a multivariate cumulative distribution function which is used to describe the dependence between random variables. In our study, we have used a gaussian copula for incorporating the joint probabilistic description of the significant wave height, water level, and wave period, also under future hydraulic conditions. The gaussian copula is an elliptical copula and it can be easily generalized to a higher number of dimensions. The main advantage of copulas is that we can generate data from multivariate distributions when there are complicated relationships among the variables, or when the individual variables are from different distributions. Copulas can be used when the marginal distributions are either parametric distributions or nonparametric distributions. To simulate correlated data, we have used gaussian copula. An n-dimensional gaussian copula according to Greene, et al. (2011) is defined by

$$C(u_1, u_2, \dots . u_n | P') = \Phi_{P,}[\Phi^{-1}(u_1), \Phi^{-1}(u_2), \dots . , \Phi^{-1}(u_n) | P'] \quad (2.2)$$

Where C indicates the gaussian copula, Φ^{-1} is the one-dimensional inverse standard normal CDF, $\Phi_{P,}$ is the joint normal n- variate CDF, u_i is a uniform random variable on [0,1] and is equal to $H_{X_i}(x_i)$, an arbitrary marginal CDF of the random variable X_i and P'

is the reduced correlation matrix of ξ_i, $i = 1,2,3, \dots n$ standard normal variables are given by

$$\xi_i = \Phi^{-1}(H_{x_i}(x_i)) \tag{2.3}$$

Φ_P, is solved by integrating the joint normal PDF $\phi_{P'}$ which is defined as follows

$$\phi_{P'}(x) = \frac{1}{(2\Pi)^{n/2}|P'|^{1/2}} e^{[-\frac{1}{2}(x-\mu)^T P'^{-1}(x-\mu)]} \tag{2.4}$$

Where μ is the mean vector, |.| indicates the matrix determinant and the joint CDF can be obtained by the following equation

$$\Phi_p(x) = \int_{-\infty}^{x_n} \dots \dots \int_{-\infty}^{x_1} \phi_P(x')dx', \dots, dx'_n \tag{2.5}$$

which is a well-known joint normal CDF. To be able to use arbitrary marginal distributions, a Gaussian copula can be constructed by transforming relating arbitrary marginal variables to standard uniform variables. Therefore, the gaussian copula with reduced covariance P' now becomes

$$C(u|P') = \int_{-\infty}^{\Phi^{-1}(u_n)} \dots \dots \int_{-\infty}^{\Phi^{-1}(u_1)} \phi_{p'}(u')du'_1 \dots \dots du'_n \tag{2.6}$$

There is no analytical solution to solve this integral equation. Numerical methods are available through various resources in open source and commercial software. In this work, MATLAB (2020) is used to perform the calibration and resampling of random variables from a multivariate Gaussian copula. Figure 9 is a scatter plot of observed wave height, wave period, and water level. Figure 10 shows the scatter plot of the simulated data using

gaussian copula. In figure 11 both the observed and simulated data are plotted together, and it shows the accuracy of the model in generating the correlated data.

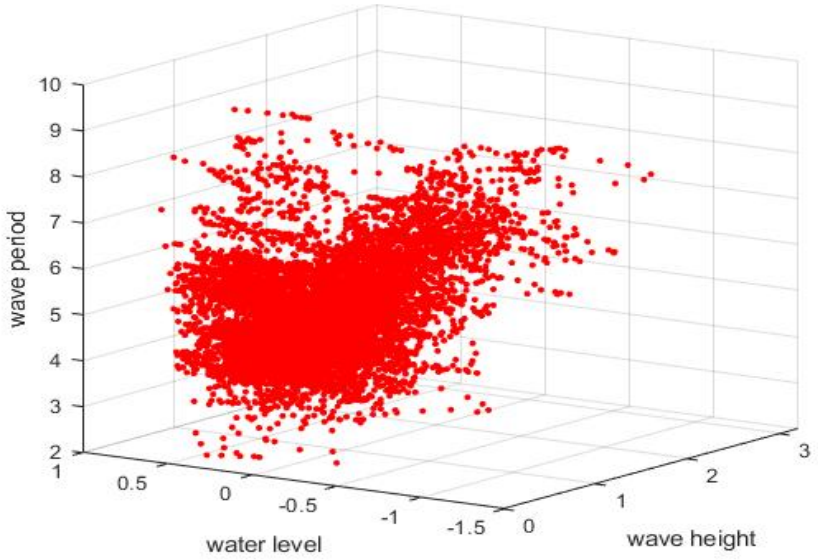

Figure 9 Scatter plot of observed water level, wave height, and period data

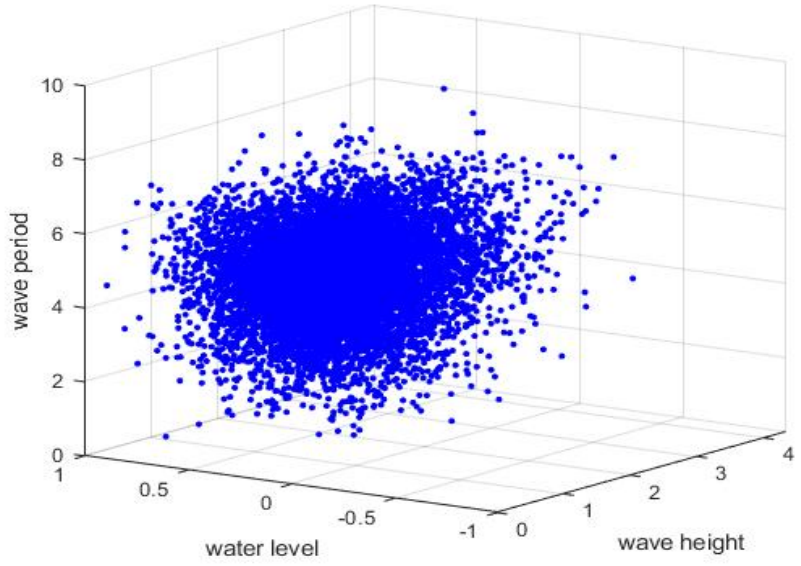

Figure 10 Scatter plot of simulated water level, wave height, and period data

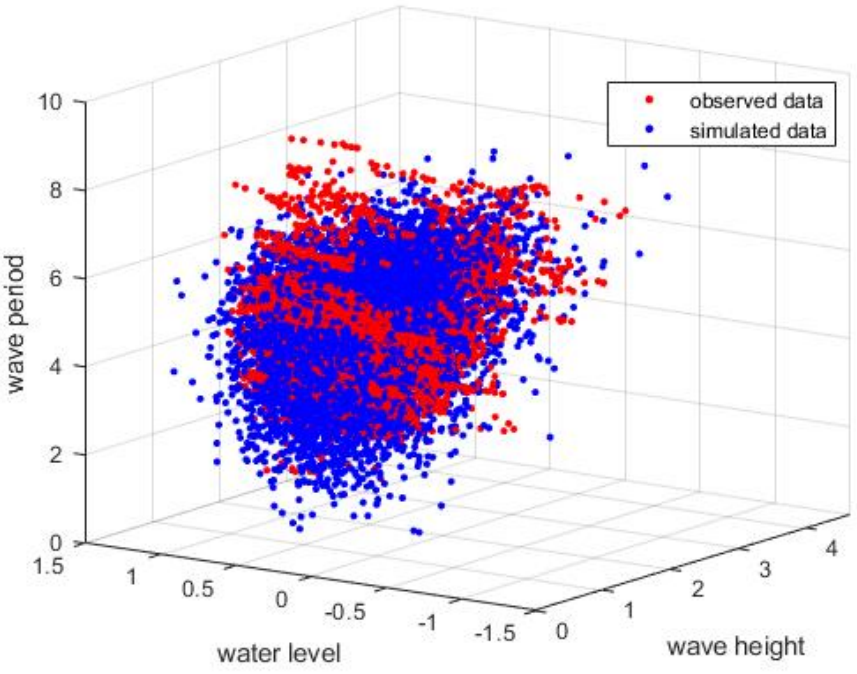

Figure 11 Combined scatter plot of observed and simulated water level, wave height and wave period data

2.6. Usage of Nonparametric Distributions

Initially, we have performed a distribution fitting analysis using parametric distributions. It is identified that among parametric distributions Weibull distribution acts as a good fit for wave height and wave period data distribution. Normal serves as a good parametric distribution fit for water level data. But it is identified that the wave height and wave period sometimes can be multimodal. To capture this property of the data we have used nonparametric distribution to fit the parameters wave height, wave period, and water level. According to Dubey, and Noshadravan, (2020). we used the kernel density estimations to define individual marginal distributions of the parameters wave height, wave period, and water level. Figure 12 shows the comparison of the nonparametric distribution and parametric distribution with observed data of wave height for the year 1997. It can be noted that through the nonparametric distributions the multimodal nature of the data is better captured than parametric distributions. Figures 13 and 14 show the comparison of parametric and nonparametric distributions with observed data of wave period and water level in which it is also evident that nonparametric distributions fit the data better than parametric distributions. Even with nonparametric distributions, copula can be used to generate the data and capture its correlation. Figure 15 represents the correlation matrix of generated and observed wave height, wave period, and water level parameters. The symmetry of the top and the bottom rectangle represents that the correlation between generated wave height, wave period and water level is similar to the correlation between those original parameters.

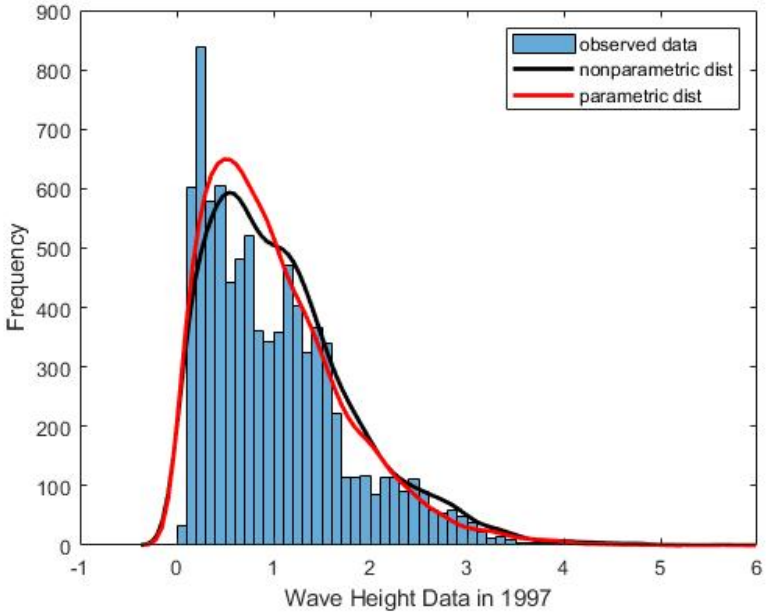

Figure 12 Comparison of nonparametric and parametric distribution fitting to wave height data

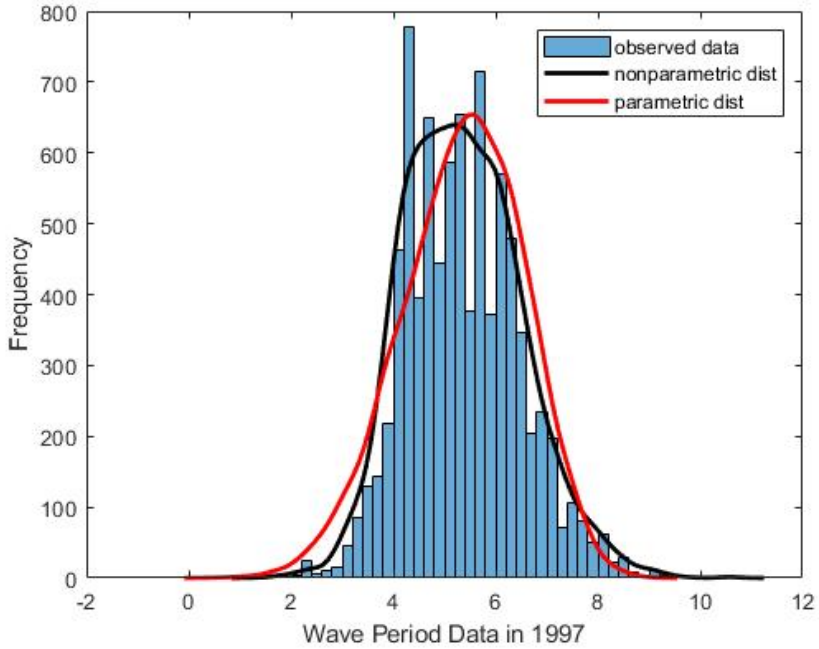

Figure 13 Comparison of nonparametric and parametric distribution fitting to wave period data

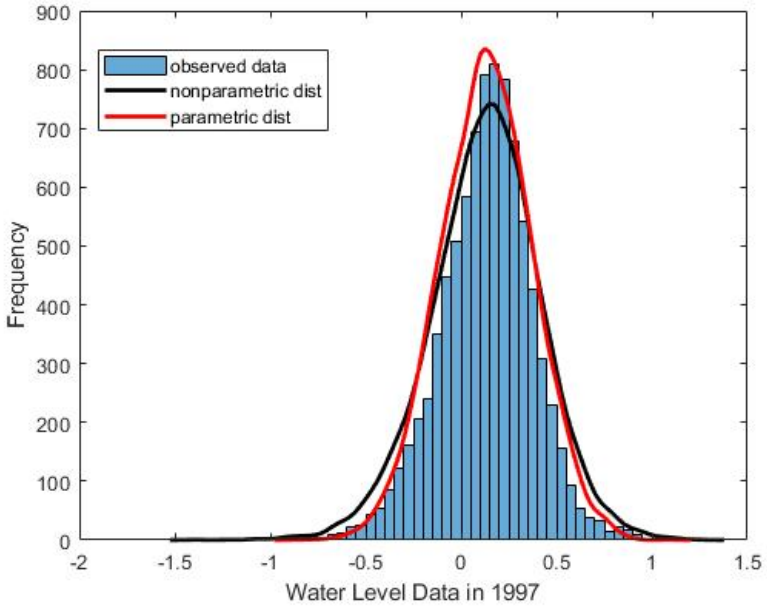

Figure 14 Comparison of nonparametric and parametric distribution fitting to water level data

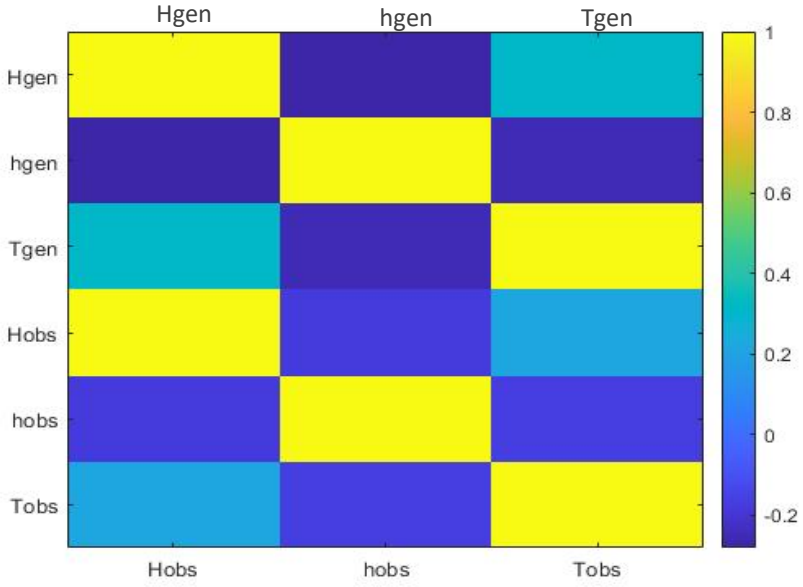

Figure 15 Correlation matrix of generated (gen) and observed (obs) wave height(H), water level(h) and wave period(T) data

3. UNCERTAINTY QUANTIFICATION OF SEA LEVEL RISE SCENARIOS

The future sea-level rise is predicted in terms of scenarios. Due to this, uncertainty arises when we want to incorporate future sea-level rise scenarios in our model. Our approach to quantifying this uncertainty is to model the sea level rise scenarios as a stochastic process. In this study, we have chosen the Inverse Gaussian (IG) process due to its advantages in incorporating random effects and its ability to model monotonic paths.

3.1. Inverse Gaussian Process

The Inverse Gaussian process is proposed by Wasan (1968). and is used as a degradation model in few studies like Wang, and Xu, (2010) and Liu et al. (2014). Ye, and Chen, (2014) have proposed three different methods to incorporate random effects; they are random drifts model, random volatility model, and random drifts- volatility model.

The inverse Gaussian process {Z(t), t>=0} is defined as the stochastic process satisfying the following.

1. Z(t) has independent increments, that is, Z (t_2) − Z (t_1) and Z (s_2) − Z (s_1) are independent $\forall t_2 > t_1 \geq s_2 > s_1$.
2. Z (t)−Z (s)follows an IG distribution with IG ($\mu(\tau(t) - \tau(s))$, $\sigma(\tau(t) - \tau(s))^2$), $\forall\ t>s \geq 0$,

Where

μ = drift parameter,

σ = diffusion parameter.

Thus Z(t) follows IG ($\mu\tau(t)$, $\sigma\tau^2$ (t)) with mean $\mu\tau(t)$ and variance μ^3 $\tau(t)/\sigma$.

Where IG ($\mu\tau(t)$, $\sigma\tau^2$ (t)) denotes the IG distribution with probability density function (PDF):

$$f(x) = \sqrt{\left(\frac{\left(\sigma\tau^2(t)\right)}{2\Pi x^3}\right)} \times exp\left(-\frac{\sigma\left(x-\mu\tau(t)\right)^2}{2\mu^2 x}\right) \quad (3.1)$$

In our study, the uncertainty in the time-evolution of future sea-level rise was quantified and systematically incorporated by constructing a stochastic model based on the inverse Gaussian process using the data from the USACE SLR projection scenarios. Inverse Gaussian process can also be extended to include unobservable factors. Unobservable factors, their effects are often represented by incorporating a random effect. Random effects models are often needed to account for unexplained heterogeneous rates within a process. In the case of SLR projections, the different scenarios (USACE high, USACE intermediate, USACE low) can be considered as heterogeneous rates within the process. Hence Inverse Gaussian process with the random-effects model makes an appropriate stochastic process for uncertainty quantification of future sea-level rise scenarios.

3.2. Application on SLR Scenarios

In figure 16 we have generated the realizations using the inverse gaussian process with random drift and compared the 5th, 50^{th,} and 95th percentiles with the original SLR curves. In figure 17 based on the SLR, we have generated water level data for some historic years and compared their probability densities with the original data. It can be observed that the simulated and observed data are not much varying.

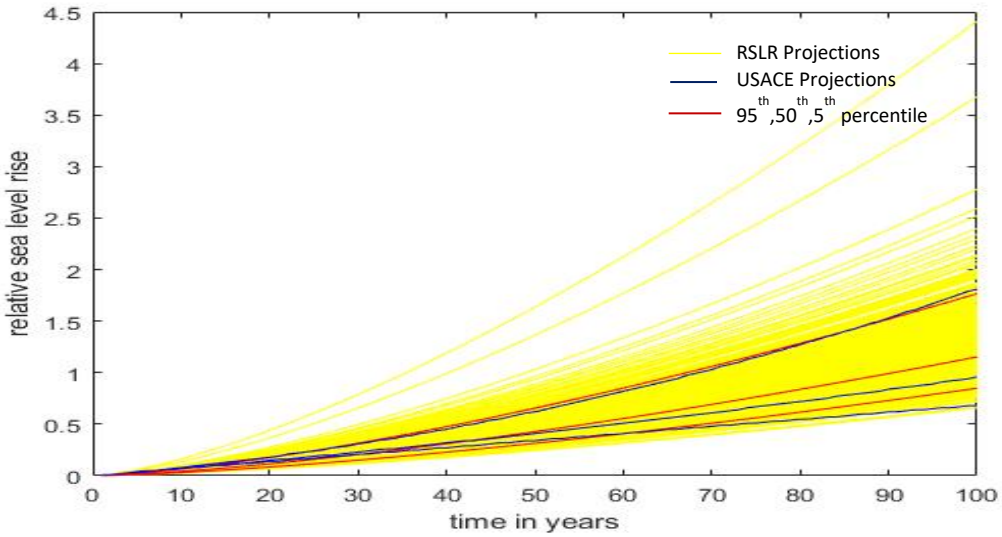

Figure 16 Realizations of RSLR scenarios generated using the inverse gaussian process

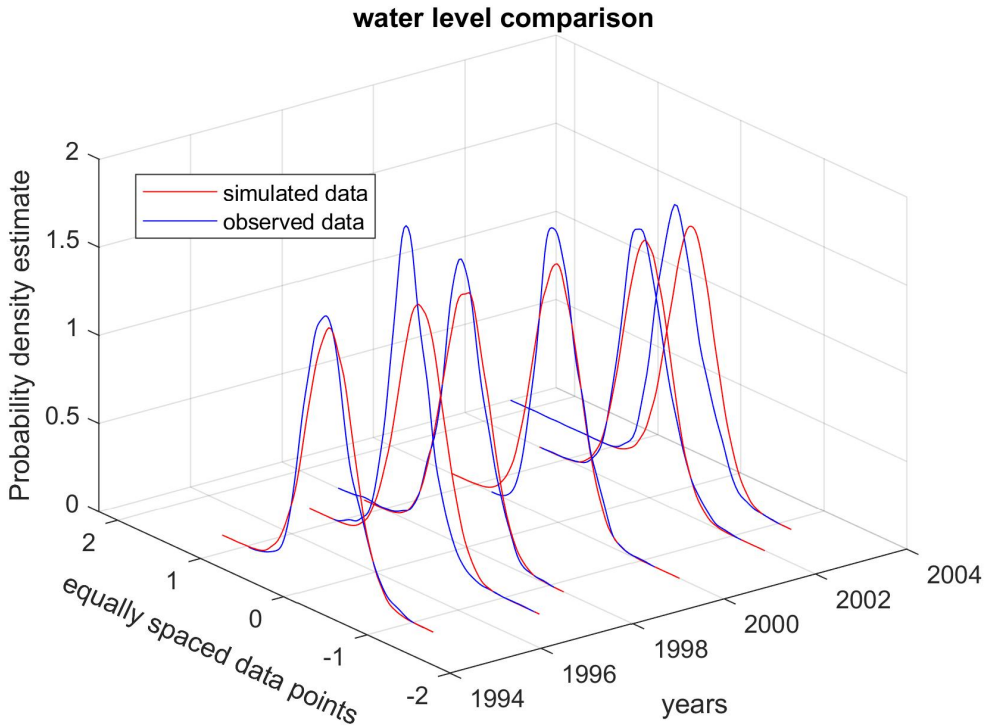

Figure 17 Comparing IG generated water level data with observed water level data for different years in the past

4. OVERTOPPING FAILURE ANALYSIS

Some of the failure modes of seawalls include overtopping failure, structural deterioration failure (due to reinforcement corrosion), teredo damage, and settlement of seawall. These failure modes depend on various factors like environmental conditions, land subsidence, materials used for the construction of the seawall, etc. Overtopping failure is considered as the most common failure mode for seawalls. Overtopping occurs when waves meet a structure lower than their approximate wave height and it is considered as the attainment of serviceability limit state. In this study overtopping failure mode is considered for risk assessment of seawall. Numerous laboratory experiments were conducted for overtopping failure study but most of them are for smooth, impermeable sloped walls. Through our study, it is identified that a significant amount of research is done on sloped and vertical sea walls, but curved sea walls are not studied extensively. So, in our analysis, we have taken a curved sea wall as a case study. USACE shore protection manual volume 2 provides ample guidance for formulating rate of overtopping for curved sea walls and it is based on some experimental evidence. It is inferred from the studies conducted by Saville (1955, 1956) on laboratory-scale models that the many factors on which the rate of overtopping discharge depends are the seawall height, shape, water depth at the toe of the seawall, slope, and whether the slope face is smooth, stepped, or rip-rapped. Small scale laboratory model tests are performed on structures of various forms by Saville and Caldwell (1953) and Saville (1955) to investigate the overtopping

rates and run-up heights. After that, a reanalysis of Saville's data helped in deriving or formulating the overtopping rate per unit length of structure which is expressed as:

$$Q = (gQ°H^3)^{1/2} exp\ (-\left(\frac{0.217}{\alpha}\right) tanh^{-1}(\frac{h - ds}{R})) \quad (4.1)$$

Or equivalently by

$$Q = (gQ°H^3)^{1/2} exp\ (-\left(\frac{0.1085}{\alpha}\right) log_e(\frac{R + h - ds}{R - h + ds})) \quad (4.2)$$

In which

$$0 \leq \frac{h - ds}{R} < 1.0$$

Where

Q = overtopping rate per unit structure length (m^3/s-m)

g = gravitational acceleration (m/s^2),

H = equivalent deep-water wave height (meters),

h = height of the structure crest above the toe of the structure (meters (m)),

ds = water depth at the structure toe (meters),

R = run-up on the structure (meters),

α and Q^o are empirically determined coefficients that depend on incident wave characteristics and structure geometry. Approximate values of α and Q^o as functions of wave steepness H/gT^2 and relative height ds /H for various slopes and structure types are given in USACE shore protection manual volume 2 (Shore Protection Manual (Vol 1 &2),

(1984)). This manual also contains guidance to account for the scale effects. In figure 18 we can visualize the parameters runup (R), water depth at the structure toe (ds), height of the structure (h), and equivalent deep water wave height (H).

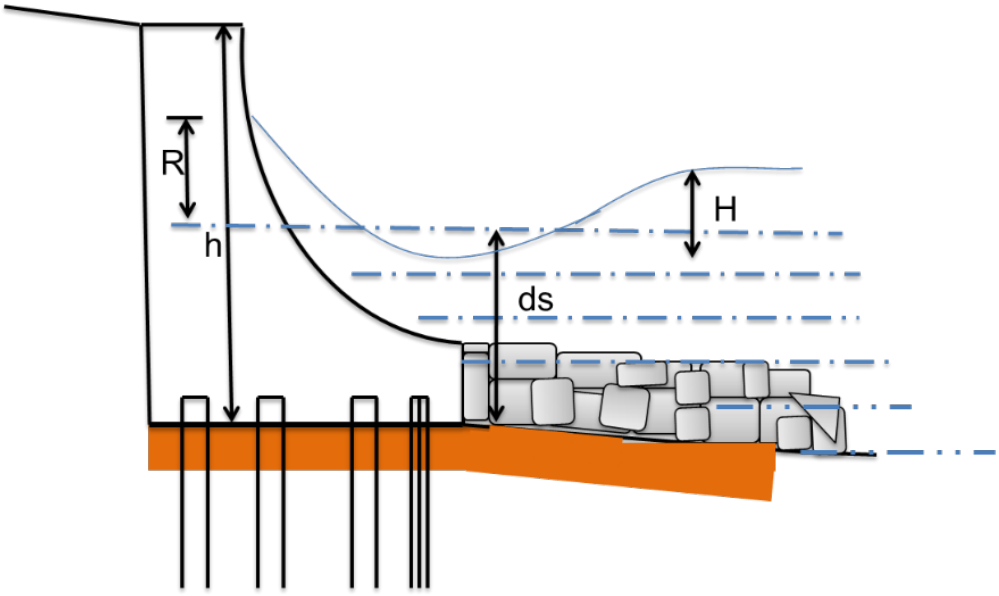

Figure 18 Galveston seawall model

By using equations 4.1 or 4.2 the overtopping rate can be calculated. To assess the risk due to overtopping first a limit state equation should be established. This limit state function as shown in equation (4.3) acts as a performance criterion.

$$F(L,S,t) = L(t) - S(t) \tag{4.3}$$

where

S(t)=action (load) or its effect.

L(t)=acceptable limit for the action or its effect; and t=time.

In the case of overtopping the term S(t) action or load is taken as the calculated overtopping rate and the term acceptable limit for the action or load is taken as the permissible overtopping rate. Usually, the permissible overtopping rate is prescribed in design codes and standards. The value of permissible discharge volume varies according to the location, geometry of the sea wall, proximity of the sea wall to the waves, and environmental conditions. The USACE coastal engineering manual part 06 contains specifications for overtopping discharge. It is based upon various studies, according to coastal engineering manual part 06 these values are considered as rough estimates and local conditions of the sea wall play an important role in deciding the permissible discharge volume. Monte Carlo methods are often employed to estimate the failure probability (Melchers, (1999)). After establishing the limit state function the probability of failure due to overtopping can be calculated by using Monte Carlo simulations. Monte Carlo is a sampling procedure and it is often used to calculate the probability of failure. The probability of failure is calculated from the number of failures generated (Chen, and Alani, (2012)). By calculating the probability of failure, we can assess the risk faced by seawalls due to overtopping.

5. IMPLEMENTATION AND RESULTS

The proposed methodology to perform time-dependent reliability assessment of seawalls exposed to stochastic waves and the rising seawater level is as follows:

5.1 Implementation

The primary and the most common mode of failure for a seawall is the overtopping failure. The main objective here is to revisit the risk faced by the seawalls over their lifetime by taking into consideration all the uncertainties involved in the process like sea-level rise and stochastic waves. To achieve this objective, we need to find the probability of overtopping failure. The important parameters in this process are wave height, wave period, and water level. Basing on sections 2 and 3 we have all the data available to perform the probability of failure analysis of overtopping. To find this probability of failure we need to formulate the limit state function. The limit state function acts as a performance criterion in assessing the risk of failure modes. For example, in the case of overtopping, permissible discharge volume (acceptable limit of action (Load))) and the magnitude of actual discharge volume (action (Load)) are taken as the two quantities of the limit state function. The calculation of actual discharge volume is based on the reanalysis of the laboratory experiments conducted by Saville as discussed in section 4. From the data analysis it is identified that correlation exists between significant wave height, period, and water levels, gaussian copulas are used for incorporating the joint probabilistic description of the seawater level and significant wave height also under the future hydraulic conditions. USACE (United States Army Corps of Engineers) SLR

scenarios and USGS (United States Geological Survey) wave projections are used to account for the future hydraulic conditions as discussed in section2 and 3. The uncertainty in the time-evolution of future sea level is quantified and systematically incorporated by constructing a stochastic model based on the inverse Gaussian process using the data from the USACE SLR projection scenarios as discussed in section 3. The inverse gaussian process with a random drift model is used for stochastically generating the sea level rise scenarios. Random effects can be incorporated into the inverse gaussian process through these random-effects models like random drift model, random volatility model, and random drift volatility model. These models help to incorporate heterogeneous rates into the model. EM algorithm is used for statistical inference of the parameters of the IG process Ye and Chen (2014) . By using Monte Carlo simulations, the failure probability of the sea wall is calculated as shown in equation 5.1. In which J=1 to N is the number of simulations, Z is the limit state function, I represents the indicator function which takes the values of unity or zero, L(t) and S(t) represent the acceptable limit for the load and the actual applied load on the structure. In the case of overtopping as discussed above it would be permissible discharge volume and calculated discharge volume or overtopping rate of the structure.

$$p_f(t) \approx \frac{1}{N}\sum_{J=1}^{N} I\{Z[L(t),S(t)] \leq 0\} \tag{5.1}$$

A schematic representation of the methodology is shown in figure 19.

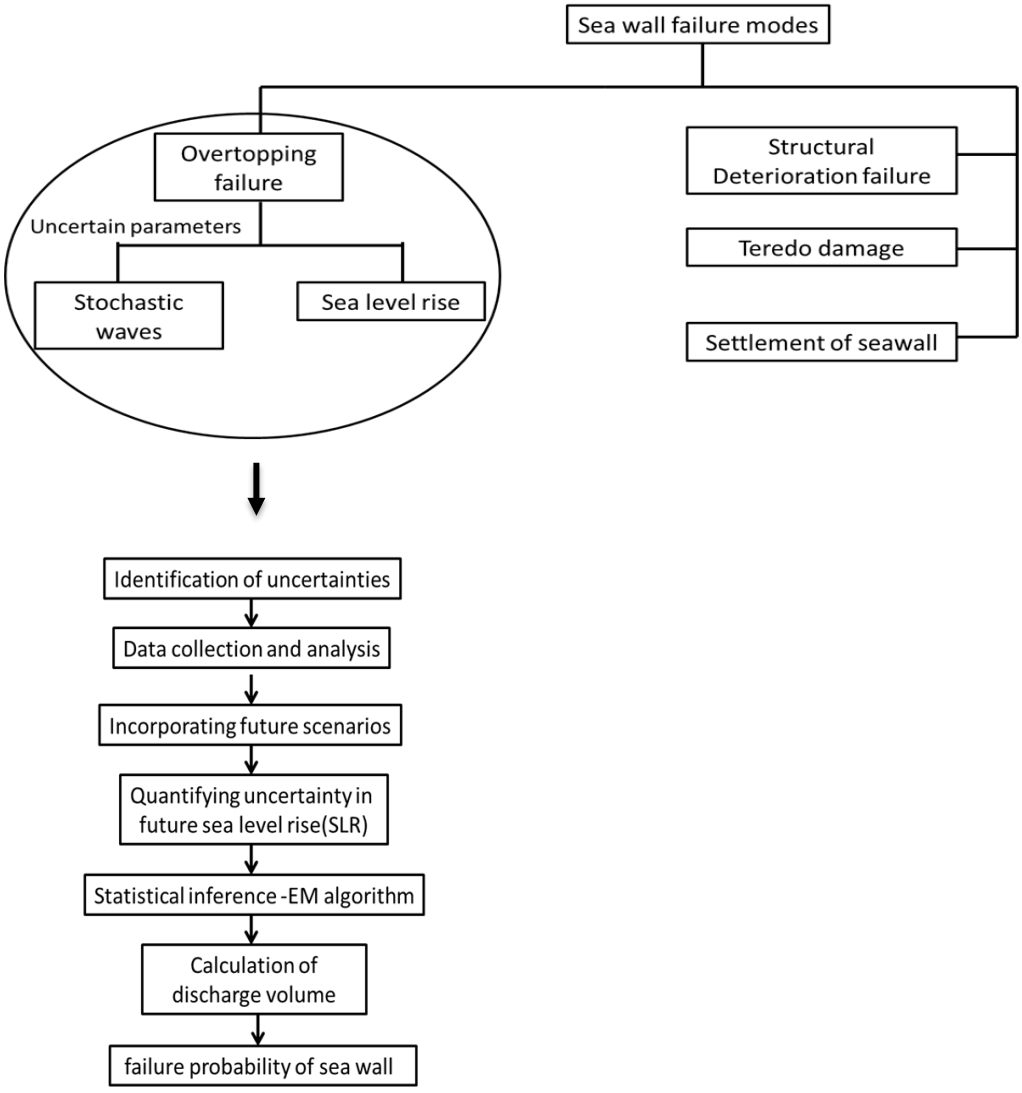

Figure 19 Schematic representation of the methodology

We have selected the Galveston seawall for our case study to apply our model. An overview of the Galveston seawall is described in the next section.

5.2 Overview of Galveston Sea Wall

The city of Galveston was hit by the most devastating hurricane in 1900 with storm tides as high as 15 ft. The damage caused by this hurricane is prolific and

according to Davis Jr, (1951). there was Property damage of $25000000 and loss of more than 6000 lives. The city responded after the storm and appointed the Robert Board to protect the city from such sea storminess. The Robert board proposed construction of the sea wall, rising of city grade and construction of an embankment 200 ft behind the sea wall and 18 ft (actual 16.6ft) above mean low water. In 1904 the sea wall construction was completed according to the proposed design. The construction details of the sea wall are as follows according to Baker, (1986): Wooden pilings were used as a foundation for the seawall. As wood is susceptible to damage due to seawater, sheet pilings were used for shielding from the water. Stone riprap was placed in the front to further protect from the damage due to moisture exposure and it is 3 feet thick and 27 feet wide in dimensions. For the construction of the concrete portions of the seawall first, a concrete substructure 16 feet wide and 3 feet thick was poured to provide a base for the section to be situated above it. The top portions of the seawall were constructed in 50-foot interlocking sections. For the reinforcement of the seawall, they adopted 1-1/4-inch steel rods.

The sea wall was subjected to its first test during the 1909 storm. The height of the tide was 6.6 ft and a considerable amount of water was thrown over the sea wall. The damage that occurred was that of the scouring of the slope of the sand embankment behind the sea wall and the riprap was lowered. Repair work was done by raising the embankment to 18 ft and toe of the sea wall was repaired by placing the riprap. In 1915 the city saw another severe storm which is as severe as the 1900 storm. But the sea wall stood strong for its purpose and saved the city from a lot of

damage compared to the 1900 storm. The Property damage was $4500000 and the loss of 12 lives. During this storm, there are tides of 14 ft above mean low water and the wave crests of about 21 ft. Damage also occurred along the foot of the sea wall due to scouring and the riprap was undermined in many locations exposing it to teredo damage. The most extensive damage was the erosion of the embankment at the back of the sea wall by a great quantity of water that was thrown over the sea wall. There was extensive damage to the embankment road and sidewalk behind the sea wall. Repair works were done by Paving on top of the embankment. The next storm occurred in 1919. During this, there was a tide 9 foot above mean low tide. The volume of water thrown over the seawall is not large and there was little damage behind the sea wall. The sea wall was subjected to extensions many times and after all the extensions the total length of the sea wall is 10.04 miles. In 1961 Hurricane Carla struck the city. The tide was 10.7 ft above mean low tide. There was partial flooding on the unprotected bayside, but the sea wall protected the city from storm wave damage. No homes were damaged, and no lives lost due to storm surge. The sea wall was also subjected to settlement and it ranges from 0.1 ft to 1.45 feet. This is an overview of the Galveston seawall and some of the storms it faced so far. Identifying the uncertainty that arises in the safety of the seawall due to future scenarios of extreme climate events and SLR we have performed a time-dependent reliability assessment to find out the impact of stochastic waves and sea-level rise on the sea wall.

5.3 Results

We have selected the Galveston sea wall model, which is a reinforced concrete curved seawall, for the case study and application of this model. A representation of Galveston seawall can be seen in figure 18. The historical and future projections of significant wave heights, periods, and water levels specifically for the Galveston region can be obtained from the USGS wave and wind projections along the US coast, NOAA, and sea level calculator of the USACE. Statistical analysis is performed on the data to characterize its distributions and other inherent properties like correlation and stationarity. Then the overtopping rate and probability of failure are calculated according to chapter 4. In figure 20 the probability of failure due to overtopping for the period 1987-2004 is plotted and it is plotted for a different number of Monte Carlo simulations. It can be observed that for a higher number of Monte Carlo runs the probability values are converging. Another inference which we can make is that the probability of failure does not follow a linear trend and there are peaks and depressions in particular years. We concluded that these peaks are due to higher wave heights occurring in those years. In figures 21,28,29 we can see the mean wave height, wave period, and water level with respect to time. Figure 22 is used to visualize the wave height data in the form of box plots. From figures 21,22 it is noted that the years with high mean wave heights had a high probability of failure. This represents the importance of wave heights when assessing the risk due to overtopping.

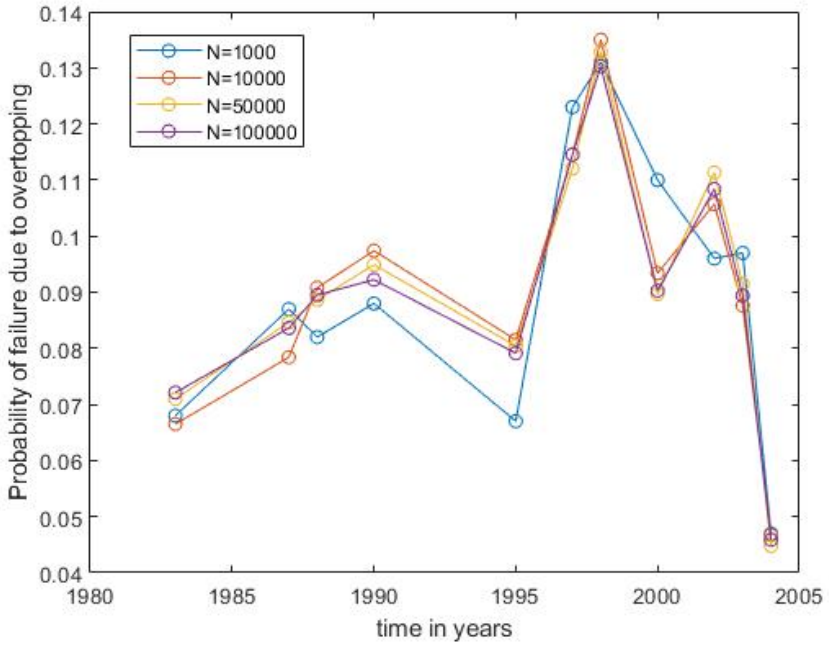

Figure 20 Probability of overtopping failure for the period 1987-2004

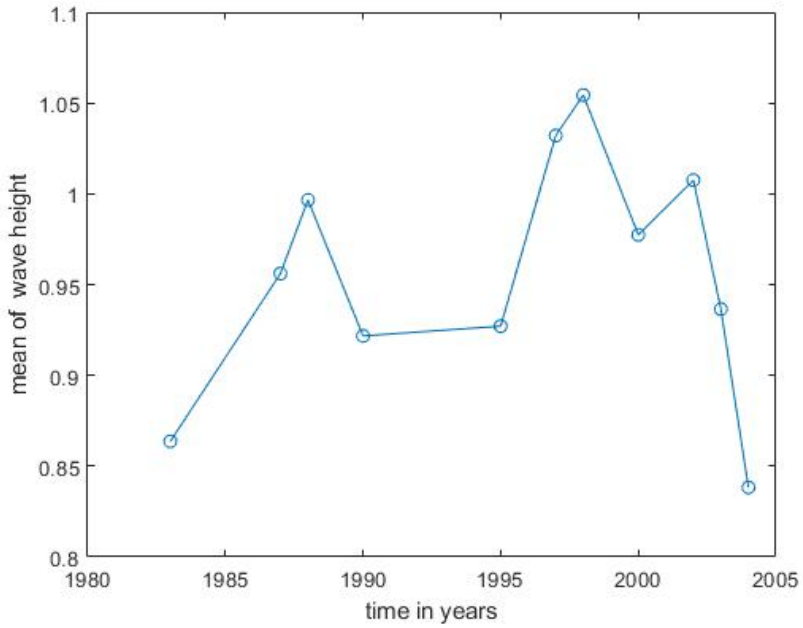

Figure 21 Mean of wave height vs time in years for the period 1987- 2004

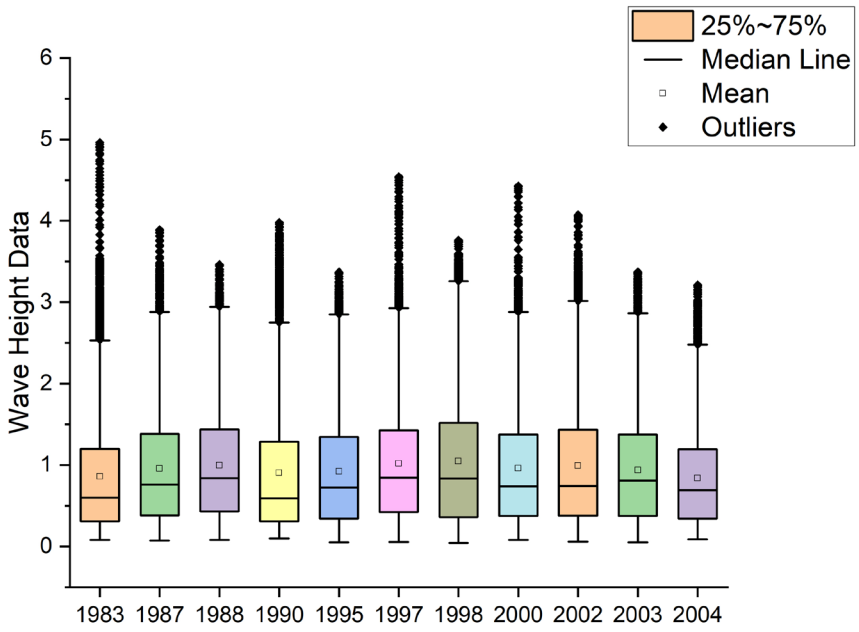

Figure 22 Boxplot for wave height data

In figure 23 the probability of failure due to overtopping is plotted with data that is generated with correlation and without correlation. It can be observed that in the uncorrelated case the probability of failure values is very much underrepresented than the original. It is observed that the simulated probability of failure using correlated data even though better than the uncorrelated result is still lower than the observed probability of failure. Investigating the reason for this discrepancy, it is identified that some of the extreme values that are present in the original data are not captured when the wave height is fitted to a simple Weibull distribution. It can be observed in figures 30, 31, 32 where the probability density of wave height, period, and water levels are compared with the original data that especially at the tail region the multimodal nature of the original data is

not completely captured through parametric distributions. To substantiate this in figures 33,34,35 boxplots are created comparing the original data and the generated data using parametric distributions which supports the same reason.

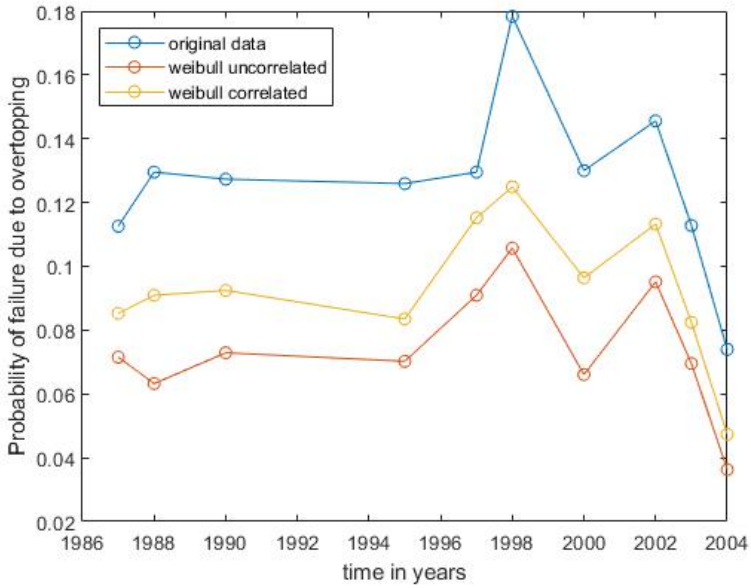

Figure 23 Probability of overtopping failure with correlated and uncorrelated data

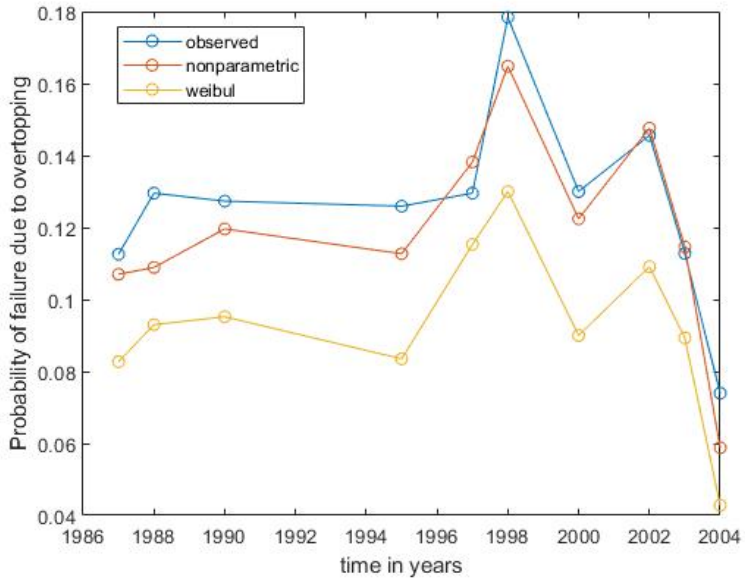

Figure 24 Comparison of overtopping probability of failure with observed data and simulated data generated by using parametric and nonparametric distributions

In figure 24 we have used nonparametric distributions to calculate the probability of failure. As discussed in section 2.6 nonparametric distributions gives a better result when compared to parametric distributions and closer to the original result. Using the data from USGS wave projections and the USACE sea-level scenarios the probability of failure for the period 2026-2038 and the period 2082-2100 are plotted and the results can be seen in figures 25 and 26. It is observed that during the period 2081-2100 the probability of failure is around 16 to 34 percent which is higher than both the periods that are the historical period and the midcentury period that is 2026-2038 period. We have plotted the probability of failure for different values of permissible discharge volume in figure 27. It is observed that the probability of failure is high when permissible discharge volume is low representing that the chance of high overtopping rate is lower.

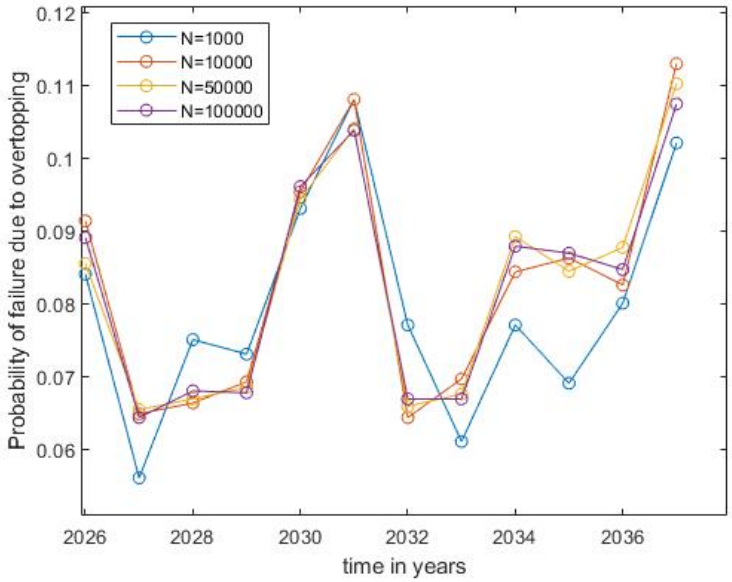

Figure 25 Probability of overtopping failure for the period 2026-2038

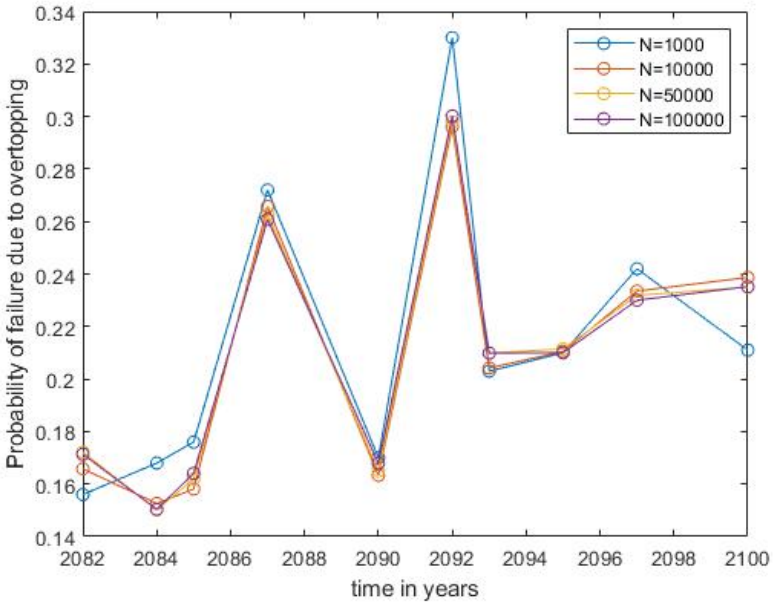

Figure 26 Probability of overtopping failure for the period 2082-2100

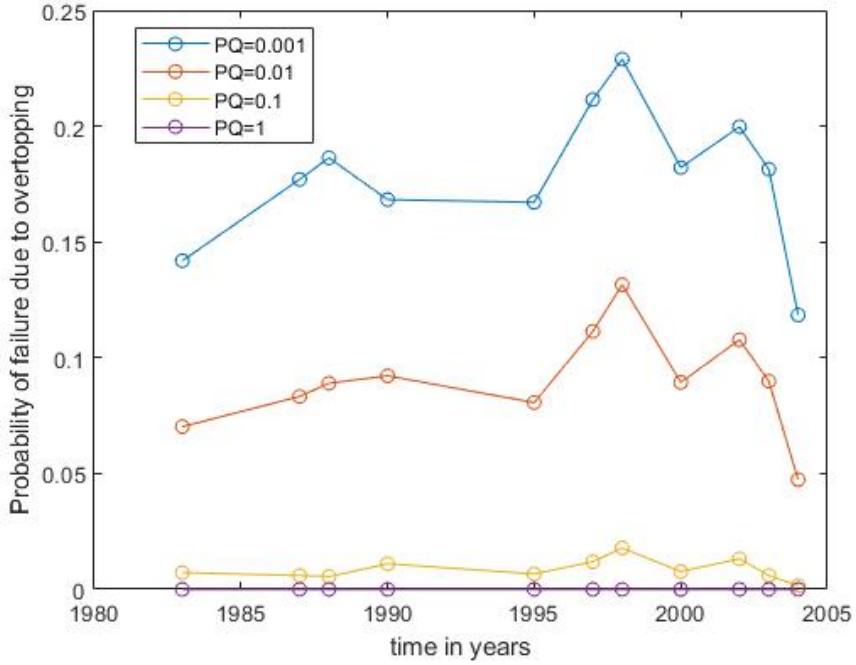

Figure 27 Probability of overtopping failure for different values of permissible discharge volume

6. CONCLUSION

In this research, we developed a risk analysis framework that uses a reliability-based approach to address the risk faced by coastal structures like seawalls especially due to overtopping. These structures are constantly subjected to stochastic waves and sea-level rise which eventually increases the coastal forcing on the structure with time. The uncertainty is unavoidable in this process originating from the stochastic nature of coastal forcing, as well as the various uncertain future scenarios of extreme climate events and sea-level rise (SLR). In our reliability analysis, we consider the uncertainty due to the stochastic nature of waves acting on the structure as well as the sea-level rise. The risk of overtopping failure is evaluated while incorporating the joint probabilistic description of the seawater level, significant wave height, and wave period, also under future hydraulic conditions. Copula is used to capture the correlation between the variables wave height, wave period, and water levels. We have integrated different data sources such as NOAA, USGS, and USACE leading to improved uncertainty quantification. The inverse gaussian process captured the uncertainty that arises due to the presence of different sea-level rise scenarios. A curved sea wall is selected as a case study to apply our model which is similar to the Galveston sea wall. The results suggest that extreme wave heights can increase the rate of overtopping. The years with high mean wave height resulted in having a high probability of failure due to overtopping representing that the effect of wave height is dominant on the probability of overtopping failure. The results when generated without correlation appeared to occur far less accurately than the original probability of failure,

signifying the importance of correlation as included in our model. The slight discrepancy that arises between the original probability of failure and the calculated probability of failure using parametric distributions is identified to be due to the inability of the parametric model to capture some of the extreme wave events. By using nonparametric distributions for the input parameters, we are able to obtain a better result compared to parametric distributions. We are able to predict the probability of failure due to overtopping for the mid-century (2026-2038) and the end of the century (2081-2100). The results suggest that the probability of failure for the end of the century is very high compared to the mid-century and the historical period. Defining the permissible discharge volume is an important factor in assessing the probability of failure as can be seen from our results that an increase in permissible discharge volume causes a decrease in the probability of failure.

In this study, we were able to quantify the risk due to overtopping failure. A seawall might be subjected to different types of failures depending on the type, location, and material of the sea wall. The other failure modes of seawall include teredo damage which is the deterioration of wooden piles exposed to seawater, settlement of seawall and structural deterioration due to reinforcement corrosion. So, a comprehensive study of all possible failure modes of a seawall over its lifetime and finding its total probability of failure as a function of system reliability can be a scope for future research work. It is also identified that understanding the bathymetry of the location and consideration of the effects of winds and wave height attenuation might lead to more accurate results in the estimation of the probability of overtopping failure.

REFERENCES

1. Baker, T. L. (1986). *Building the Lone Star: An Illustrated Guide to Historic Sites* (No. 20). Texas A & M University Press.
2. Burcharth, H. F., Maciñeira, E., & Noya, F. (2015). Design, construction, and performance of the main breakwater of the new outer port at Punta Langosteira, A Coruña, Spain. *Design of Coastal Structures and Sea Defenses*, 23-76.
3. Chen, H. P., & Mehrabani, M. B. (2019). Reliability analysis and optimum maintenance of coastal flood defenses using probabilistic deterioration modeling. *Reliability Engineering & System Safety*, *185*, 163-174.
4. Chen, H. P., & Alani, A. M. (2012, June). Reliability and optimized maintenance for sea defenses. In *Proceedings of the Institution of Civil Engineers-Maritime Engineering* (Vol. 165, No. 2, pp. 51-64). Thomas Telford Ltd.
5. Coastal Engineering Research Center (US). (1984). *Shore Protection Manual (Vol 1 &2)*. Department of the Army, Waterways Experiment Station, Corps of Engineers, Coastal Engineering Research Center.
6. Davis Jr, A. B. (1951). *Galveston's bulwark against the sea: history of the Galveston seawall*. US Army Corps of Engineers, Galveston District.
7. Dubey, V., & Noshadravan, A. (2020). A probabilistic upscaling of microstructural randomness in modeling mesoscale elastic properties of concrete. *Computers & Structures*, *237*, 106272.
8. Engineers, U. A. C. O. (2002). Coastal Engineering Manual. Engineer Manual

1110-2-1100. *US Army Corps of Engineers, Washington, DC*.

9. Erikson, L.H., Storlazzi, C.D., Barnard, P.L., Hegermiller, C.E., and Shope, J.B., 2016. Wave and Wind projections for United States Coasts; Mainland, Pacific Islands, and United States-Affiliated Pacific Islands. U.S. Geological Survey data release, http://dx.doi.org/10.5066/F7D798GR

10. Greene, M. S., Liu, Y., Chen, W., & Liu, W. K. (2011). Computational uncertainty analysis in multiresolution materials via stochastic constitutive theory. *Computer Methods in Applied Mechanics and Engineering*, *200*(1-4), 309-325.

11. Huber, M., & White, K. (2017). Sea level change curve calculator (2017.55) user manual. *US Army Corps of Engineers. Retrieved from http://www. corps climate. us/docs/Sea_Level_Change_Curve_Calculator_User_Manual_2017_55_FINAL. pdf*.

12. Li, C. Q., & Zhao, J. M. (2010). Time-dependent risk assessment of combined overtopping and structural failure for reinforced concrete coastal structures. *Journal of waterway, port, coastal, and ocean engineering*, *136*(2), 97-103.

13. Li, C. Q., Lawanwisut, W., & Zheng, J. J. (2005). Time-dependent reliability method to assess the serviceability of corrosion-affected concrete structures. *Journal of structural engineering*, *131*(11), 1674-1680.

14. Liu, Z., Ma, X., Yang, J., & Zhao, Y. (2014). Reliability modeling for systems with multiple degradation processes using inverse Gaussian process and copulas. *Mathematical Problems in Engineering*, *2014*.

15. Lounis, Z., & Amleh, L. (2004). Reliability-based prediction of chloride ingress and reinforcement corrosion of aging concrete bridge decks. In *Life-Cycle Performance of Deteriorating Structures: Assessment, Design and Management* (pp. 113-122).

16. MATLAB. (2020), R2020a, The MathWorks Inc. Natick, MA, USA. https://www.mathworks.com/

17. Mehrabani, M. B., & Chen, H. P. Markov Chain modelling for life-cycle performance assessment of coastal flood defences.

18. Mehrabani, M. B., Chen, H. P., & Stevenson, M. W. (2015). Overtopping failure analysis of coastal flood defences affected by climate change. In *Journal of Physics: Conference Series* (Vol. 628, No. 1, p. 012049). IOP Publishing.

19. Melchers, R. E. 1999,'Structural Reliability Analysis and Prediction', John Wiley & Sons. Chichester, England.

20. Muraleedharan, G., Nair, N. U., & Kurup, P. G. (1993). Characteristics of long-term distribution of wave heights and periods in the eastern Arabian Sea.

21. Muraleedharan, G., Kurup, P. G., & Unnikrishnan Nair, N. (1998). Weibull model for shallow water wave height distribution and prediction. In *National Conference on Current Trends in Ocean Predictions with Special Reference to Indian Seas. Cochin, India* (pp. 80-85).

22. NOAA: Water Levels, Galveston Pleasure Pier, TX- Station ID: 8771510, NOAA. [URL: https://tidesandcurrents.noaa.gov/waterlevels.html?id=8771510]

23. Origin (Pro). (2020), version 2020. OriginLab Corporation, Northampton, MA, USA.

24. Panoply. (2020), version 4.11.3, NASA Goddard Institute for Space Studies, New York, NY,USA. https://www.giss.nasa.gov/tools/panoply/

25. Saville, T., & Caldwell, J. M. (1953). *Accuracy of hydrographic surveying in and near the surf zone* (No. 32). US Beach Erosion Board.

26. Saville, T. (1955). *Laboratory data on wave run-up and overtopping on shore structures* (No. 64). US Beach Erosion Board.

27. Saville, T. (1956). Wave run-up on shore structures. *Journal of the Waterways and Harbors Division*, *82*(2), 1-14.

28. Wang, X., & Xu, D. (2010). An inverse Gaussian process model for degradation data. *Technometrics*, *52*(2), 188-197.

29. Wasan, M. T. (1968). On an inverse Gaussian process. *Scandinavian Actuarial Journal*, *1968*(1-2), 69-96.

30. Ye, Z. S., & Chen, N. (2014). The inverse Gaussian process as a degradation model. *Technometrics*, *56*(3), 302-311.

31. Yoskowitz, D. W., Gibeaut, J., & McKenzie, A. (2009). The socio-economic impact of sea level rise in the Galveston Bay Region. *Corpus Christi, TX: A Report for the Environmental Defense Fund. Harte Research Institute for Gulf of Mexico Studies, Texas A&M University*.

APPENDIX A

ADDITIONAL GRAPHS

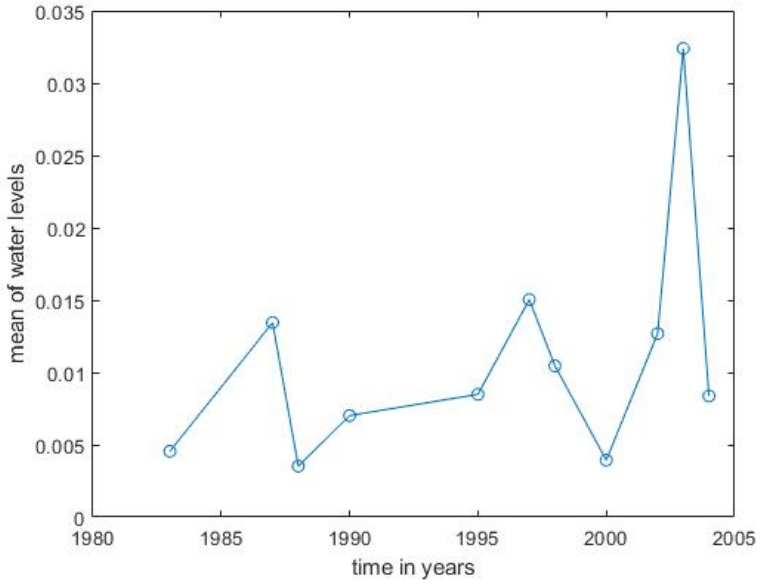

Figure 28 Mean of water levels vs time in years for the period 1987- 2004

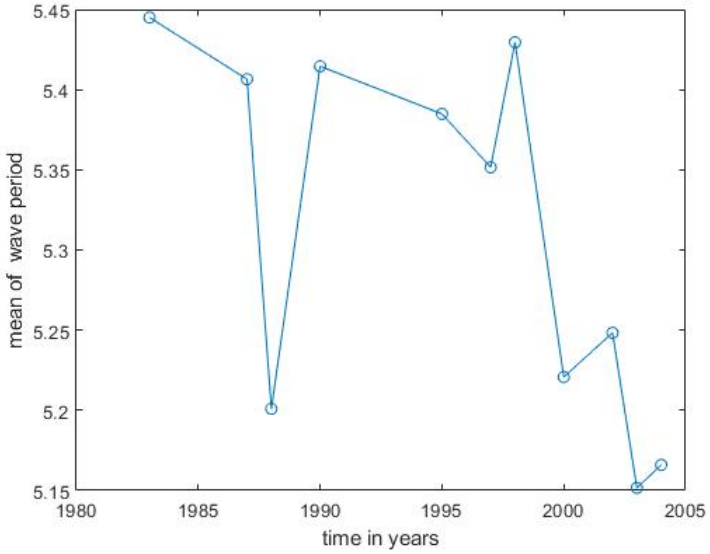

Figure 29 Mean of wave period vs time in years for the period 1987- 2004

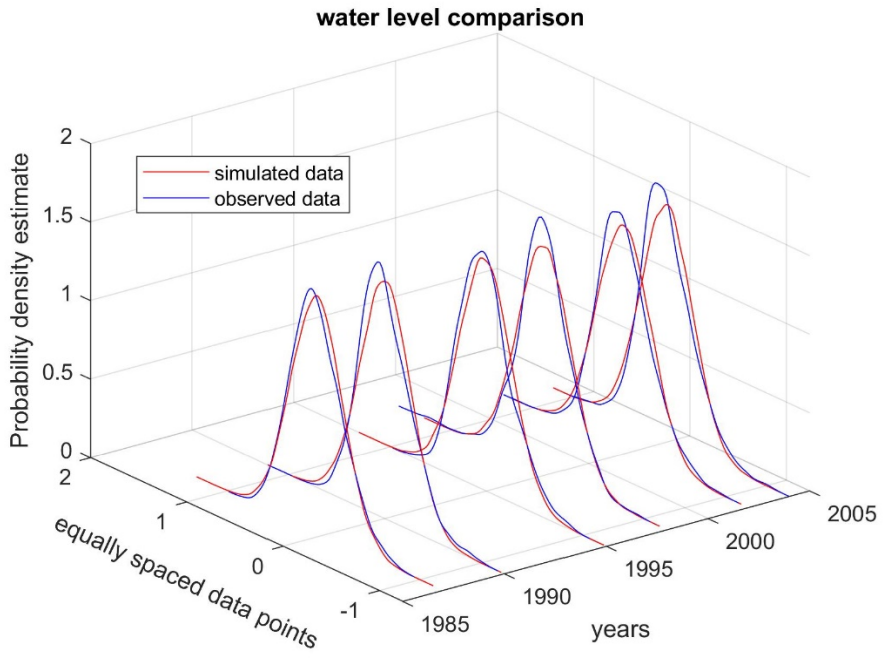

Figure 30 Comparing observed water level data and water level data simulated using parametric distribution (normal)

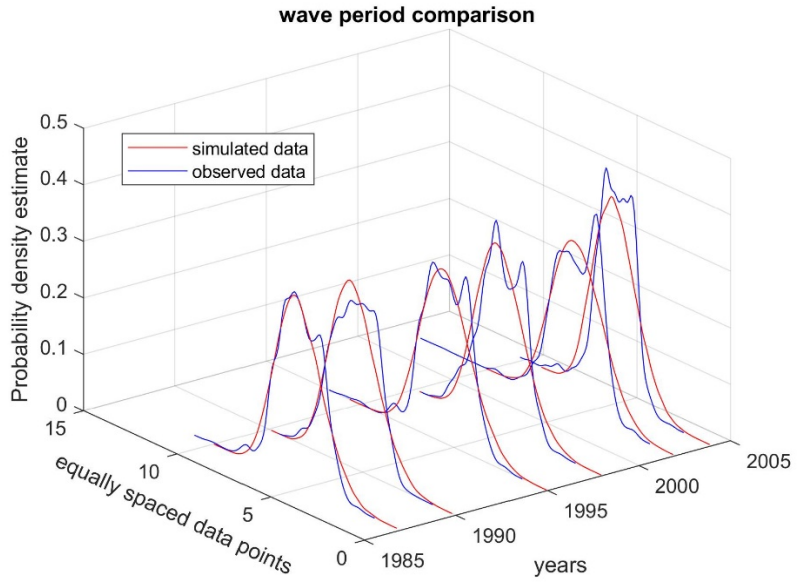

Figure 31 Comparing observed wave period data and wave period data simulated using parametric distribution (weibull)

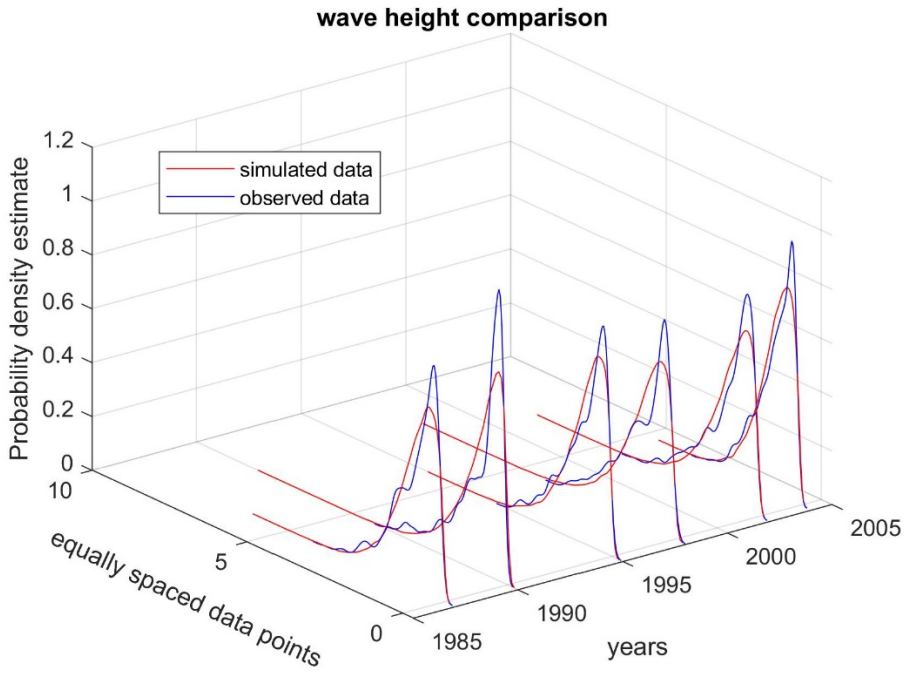

Figure 32 Comparing observed wave height data and wave height data simulated using parametric distribution (weibull)

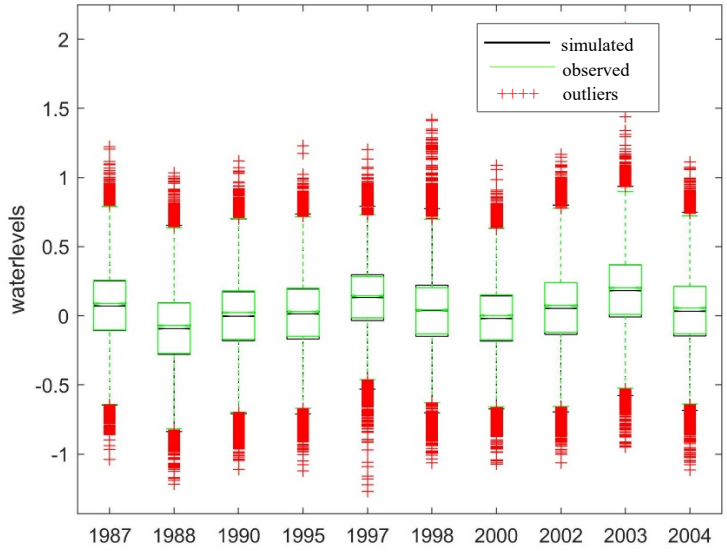

Figure 33 Box plot for water level data comparing simulated and observed data

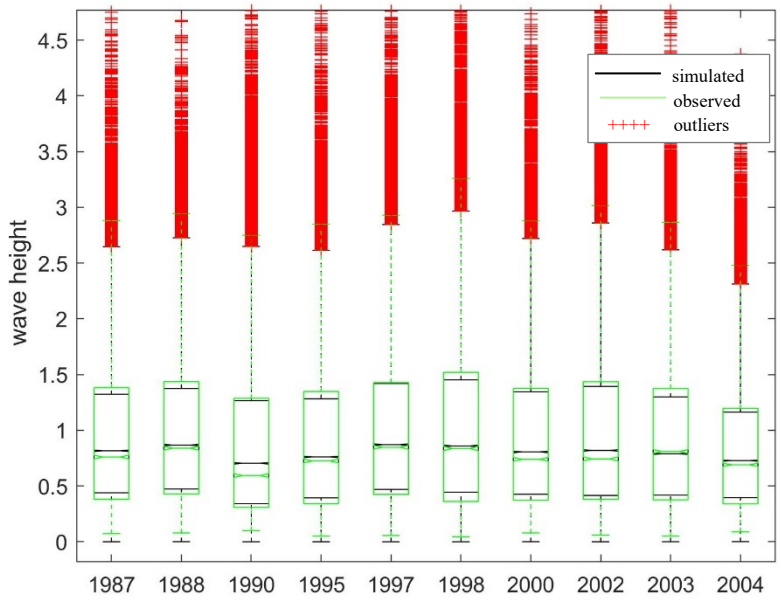

Figure 34 Box plot for wave height data comparing simulated and observed data

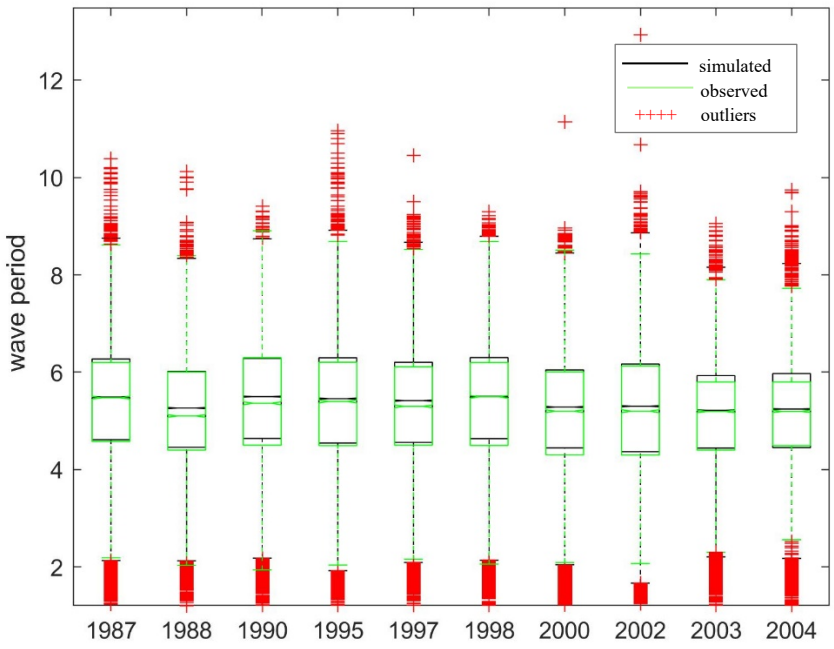

Figure 35 Box plot for wave period data comparing simulated and observed data